GENERAL DYNAMICS | ASTRONAUTICS

FREEZING OF CRYOGENIC LIQUIDS WHEN EXPANDED TO PRESSURES BELOW THE TRIPLE POINT PRESSURE

Contract NAS 3-3232

GENERAL DYNAMICS

Convair Division

ACKNOWLEDGEMENTS

Sincere appreciation is expressed to P. S. Vincelett of the Centaur Weight Control Group (966-8) for his suggestions and the many hours of help given in the design, development and operation of the test fixtures used for the Micro-Meteorite Puncture Leakage Study, and for his general contribution to the program. To the many others who offered their advice and assistance, the author is indebted.

FOREWORD

This report was prepared to document experimental studies of the freezing phenomena attending the free expansion of cryogenic liquids, specifically hydrogen and nitrogen, to pressures below the triple point pressure. Documented are two separate blocks of tests with separate objectives. The tests were performed during September 1961 and intermittant periods during 1962.

TABLE OF CONTENTS

TABLE OF CONTENTS (Continued)

LIST OF ILLUSTRATIONS

LIST OF ILLUSTRATIONS (Continued)

SUMMARY

Two experimental studies are documented in this report. The first is mainly concerned with photographically recording the freezing phenomena associated with an expansion to pressures below the triple point using various mockups of actual Centaur hardware. The second study deals with the flow characteristics of liquid hydrogen and nitrogen through simulated micro-meteorite punctures in 0.010" thick stainless steel into a pressure environment below the triple point pressure. Specifically, the coefficient of discharge associated with incompressible, ideal fluid flow was measured, and the effect of the freezing of the liquid on the flow was evaluated. The results of each study are given independently in the respective subsections.

A large percentage of the experimental results was obtained via high-speed 16 MM movie film. A listing of the film record, as well as its location, is given for each test block. Specific scenes are included in the report to give an indication of what is contained in the film record.

A thermodynamic analysis was made of the freezing phenomena to provide quantitative concurrence with that which was observed. This analysis is given in the Appendix along with development problems encountered with the Micro-Meteorite Puncture Leakage Study test fixtures.

I. INTRODUCTION

The use of cryogenic liquids as space vehicle propellants has been accompanied by difficult state-of-the-art type problems affecting the operation of the vehicle in free space. One of these problems is the freezing phenomenon associated with the free expansion of a cryogenic liquid (or cold gas) to an environment where the pressure is below its triple point pressure. Areas of uncertainty exist in parameters which control the freezing and the general phenomenon itself. In order to be able to evaluate the associated problems for any location where freezing might occur, the basic phenomenon and its effects must be known. In order to have a better understanding of the problems as associated with the Centaur vehicle, the tests documented in this report were performed. Attempts were made to simulate actual Centaur hardware as well as to investigate the visible phenomena associated with various expansion configurations.

II. HYDROGEN AND NITROGEN TESTS OF THE GENERAL FREEZING PHENOMENON ASSOCIATED WITH A FREE EXPANSION

Early in the Centaur vehicle development phase, the ignition of the main engines was immediately proceeded by a pre-start chilldown sequence which dumped oxygen directly into the Atlas/Centaur Interstage Adapter. Hydrogen was dumped overboard through the walls of the adapter through approximately a one-inch diameter duct. This chilldown sequence carried over into the Centaur staging sequence. During staging, the hydrogen overboard vent line disconnected near the walls of the adapter. At this time, liquid hydrogen was most probably being dumped into the oxygen-filled interstage adapter, which was now in a near vacuum pressure condition.

No information was available as to whether or not a combustible mixture was present or in what form the escaping hydrogen would assume when expanded to such a low pressure. Analytically it could be determined that a large portion of the liquid hydrogen would freeze, but the form it would take was a matter of conjecture. It was considered possible that, as the freezing phenomenon took place, oxygen could be entrapped with the hydrogen, forming a potentially dangerous mixture.

This block of testing, described below, further investigates this situation and the general freezing phenomena produced by an expansion to very low pressures.

A. Test Objectives

1. Study and photograph the freezing phenomena attending the free expansion of liquid hydrogen and liquid nitrogen, with various expansion configurations, to pressures below the triple point pressures.
2. Evaluate the freezing phenomenon associated with the venting of LH_2 into the Centaur/Atlas interstage adapter during the Centaur in flight pre-start chilldown sequence. No attempt was made to simulate the thermal environment.

B. Test Apparatus

The apparatus was arranged as is shown in Figure 1 and consisted of:

1. The Aerophysics Laboratory Altitude Chamber which is capable of approximately 85 statute mile altitude pressure simulation (1×10^{-5}MM Hg); it is not capable of thermal simulation.

2. Pneumatically-operated one-inch Anin valve with associated helium system and 4-way solenoid control valve.
3. Stainless steel hydrogen reservoir of approximately 0.25 ft^3 capacity. This was necessary to allow closing of the vent valve during testing to avoid the hazard of a possible combustible H_2-O_2 mixture in the chamber.
4. One-inch diameter (nominal) LH_2 ducting.
5. Necessary pressure gauges.
6. A mylar catch surface to accumulate solid. This would slow down the sublimation rate and prolong the test run time. The test was terminated when the tank pressure rose from its initial value to above 0.9939 psia, the H_2 triple point.
7. Variable orifice configuration (see Figure 2).

C. Scope of Testing

1. In support of Test Objective 1 the following orifice inserts or configurations were tested with LH_2 and/or LN_2:
   (a) The one-inch diameter exit of the Anin valve without the attached flange with LH_2 and LN_2 (Orifice No. 0);
   (b) The following orifice inserts with dimensions as shown in Figure 3:

Orifice No.	(L) Orifice Length In Inches	(D) Orifice Diameter In Inches	L/D	Material	Wall Thickness (if a capillary tube)	Fluid Used
2	2.0	0.43	4.65	S.S.	0.035"	LN_2/LH_2
3	2.0	0.18	11.1	S.S.	0.035"	LN_2/LH_2
4	2.0	0.18	11.1	S.S.	0.035"	LN_2
*	6.0	0.25	24.0	plastic plex-hose	------	
5	0.0468	0.50	0.09	alum.	------	LH_2
6	0.0625	(0.125 ea. 7 holes-6 on a 1/4" radius. Like a showerhead.)		S.S.	------	LH_2

* Used together - see Figure 3(a).

Several more orifice inserts of different materials were made up but not tested. It was thought that much more could be gained if the piece tested was transparent, since it was observed that different materials of the same orifice size exhibited (visually) essentially the same phenomena. However, other priority tests using the altitude chamber prematurely concluded the tests for this block.

(c) The following miscellaneous orifice configurations were tested:

(1) A short section of 3/4" (nominal) tubing attached to the orifice flange and capped on the bottom end with the top nut loose (See Figure 4(a) .

(2) A mock-up of a non-propulsive vent (6-1/8" diameter holes drilled diametrically opposite in a nominal 1" bulkhead fitting with a cap). See Figure 4(b) ; (It was tested with LH_2.)

(3) Nozzle for the GD/A Zero-"G" separator (0.029 in^2 throat area . See Figure 4(c). (It was tested with LH_2.)

2. In support of Test Objective 2, the following tests were performed:

(a) A mockup of the Centaur interstage adapter with a section of the "Z" shaped reinforcement member attached was constructed in simulation of the actual Centaur configuration. Stainless steel and aluminum tubing were placed across the mylar surface directly below the orifice to determine if a solid sheet of frozen hydrogen or nitrogen would build up on them. See Figure 5(a). They were tested as follows:

Orifice No.	Fluid Used	Tubes Used (X)
0	LN_2	
2	LN_2	X
3	LN_2	X
0	LH_2	X

(b) Orifice No. 5 was directed at two thin metal sheets, 0.032 thick aluminum and 0.010 thick stainless steel, which represented the interstage adapter wall and Atlas forward bulkhead. The purpose was to determine: (1) if solid H_2 would adhere to the wall; and (2) the length of impinging time required for the solid to first appear See Figure 5(b) .

D. Test Results

The procedure during the tests was to photographically record the freezing phenomena. As a result, most of the test results are recorded on movie film. Specific scenes are shown in Figures 6, 7 and 8. A listing of the film record is given in a following subsection.

In general, the visually observed results of the tests described above indicated that when a cryogenic liquid was freely expanded to a state where the pressure was below its triple point pressure, it flashed

into a gas. In order to make the transition, however, it must have been supplied with the necessary "heat of vaporization". Because the expansion occurred very rapidly, heat was essentially unavailable from exterior sources. Therefore, the liquid which flashed absorbed heat from the neighboring liquid. The result was that a small percentage of the liquid vaporized, and in doing so, froze the remainder. The author feels that the expansion caused the liquid to first break up into tiny droplets which in turn vaporized from their outside surfaces and thereby froze the interior liquid. This is because the form the solid produced from expanding through a large hole was that of a myriad of tiny particles resembling a heavy mist, as shown in Figure 6. This form was affected by: (a) the hole size (diameter and length), (b) the available heat flux from the surroundings, and (c) the pressure drop across the hole.

When the hole size was small and had a large L/D ratio, the form of the solid produced was that of a crystalline extrusion.

Both of these situations occurred only when the latent heat necessary to vaporize all of the liquid expanding through the hole was not available from the surroundings. The configurations tested produced solid as soon as the valve was opened. The valve, however, was chilled to near liquid temperatures at this time. In general, when the surroundings were unable to supply the heat necessary to allow all of the

expanding liquid to vaporize, solid would begin to appear.

The use of different materials in place of stainless steel for the same expansion configuration essentially affected only the available heat flux. After equilibrium was achieved, or in other words, after the available heat was essentially absorbed, the freezing phenomena was the same for any material. Materials in the vicinity of the solid spray (mist) and oriented such that the spray impinged upon them were chilled to a point where a solid sheet began to build up as the spray continued. The length of impinging time required before a solid sheet began to appear depended on (a) the fluid being expanded, (b) the material being impinged upon and its surroundings, and (c) the separation and orientation of the material with respect to the jet.

For the interstage adapter mockup and the stainless steel and aluminum tubing at the distances indicated in Figure 5(a), the impinging time required was approximately 5 to 10 seconds for hydrogen and 15 to 20 seconds for nitrogen. For the stainless steel and aluminum sheets shown in Figure 5(b) tested with LH_2, the impinging time for the stainless was about 5 to 6 seconds and for the aluminum was 10 to 15 seconds.

E. Film Record

The usable film of the hydrogen expansion studies in this block of testing has been edited, compiled and separated with titles into one

film reel entitled "Liquid Hydrogen Expansion Test". This is kept on file by the Motion Pictures and Television Group, Dept. 120-4. The originals of all the film taken in this block of testing are also kept on file by the same Department under the general title of "Vacuum Valve Test".

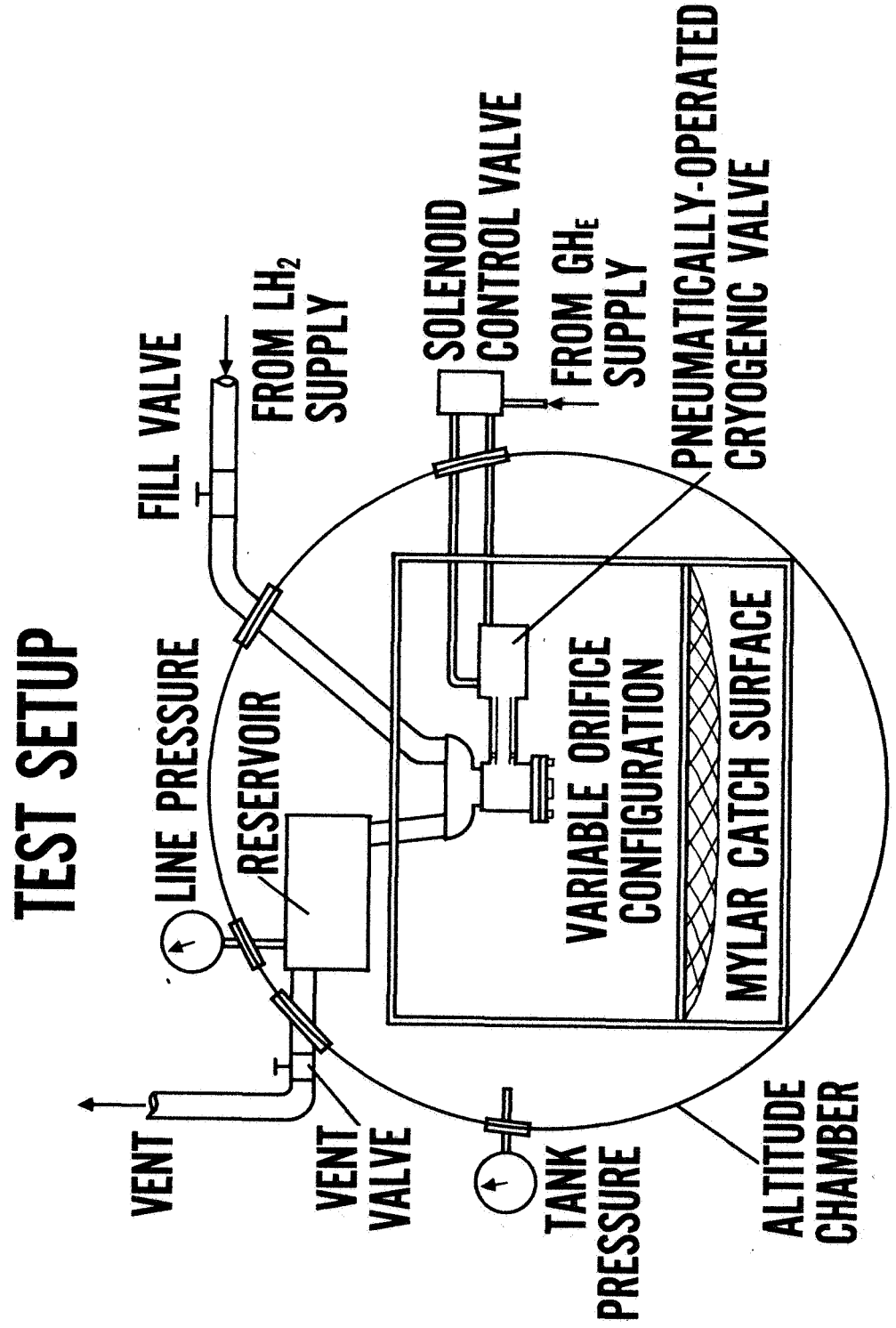

FIGURE 1
Hydrogen Expansion Test Schematic

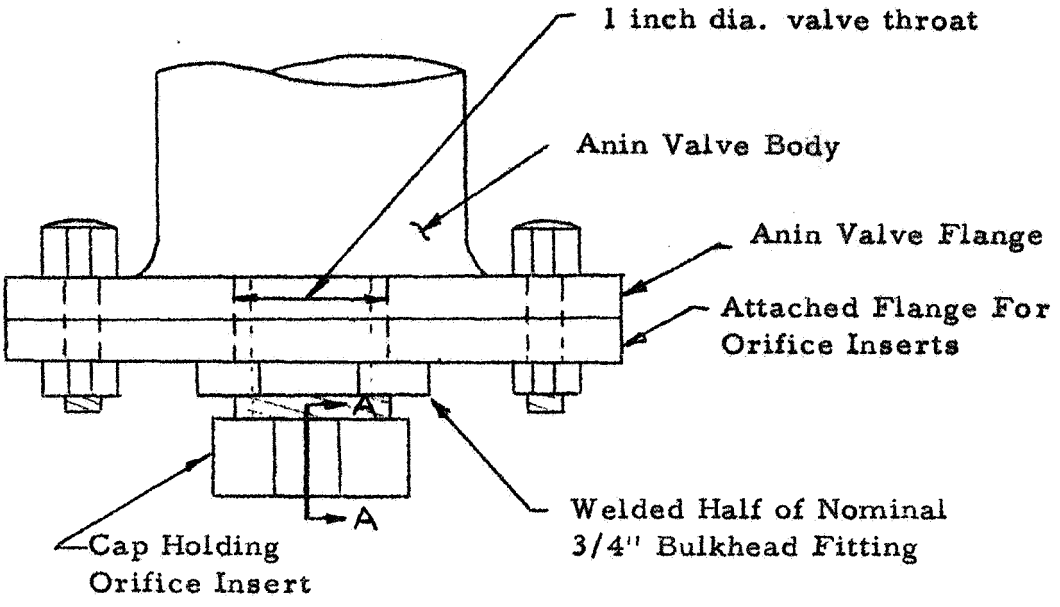

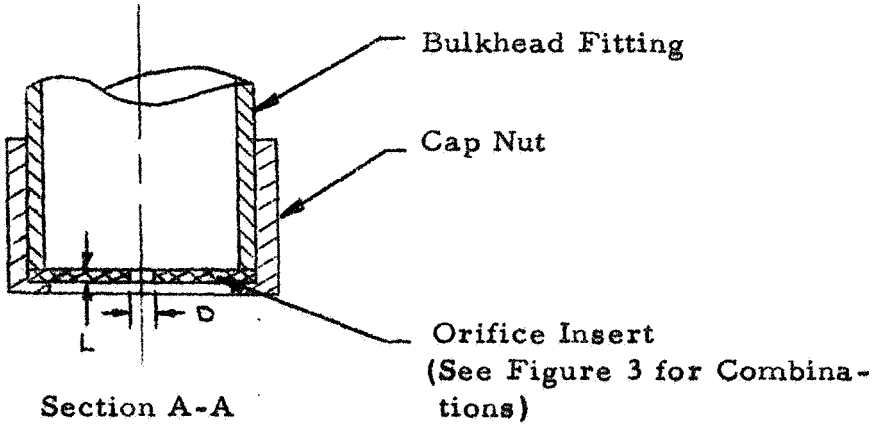

FIGURE 2

Variable Orifice Configuration

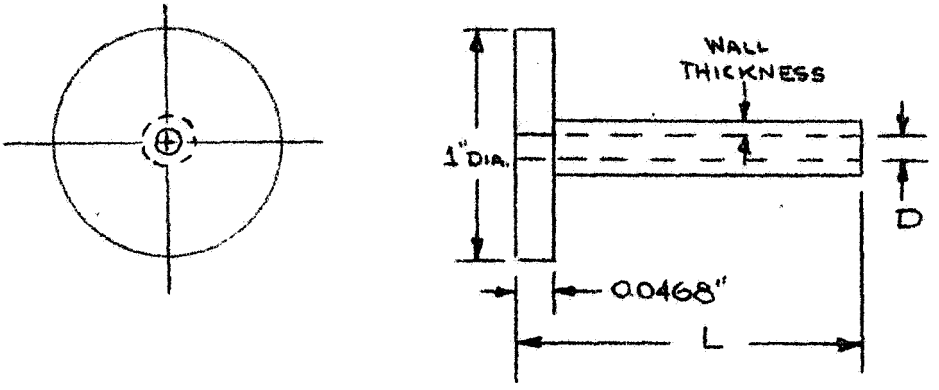

FIGURE 3a
Orifice Insert General Schematic

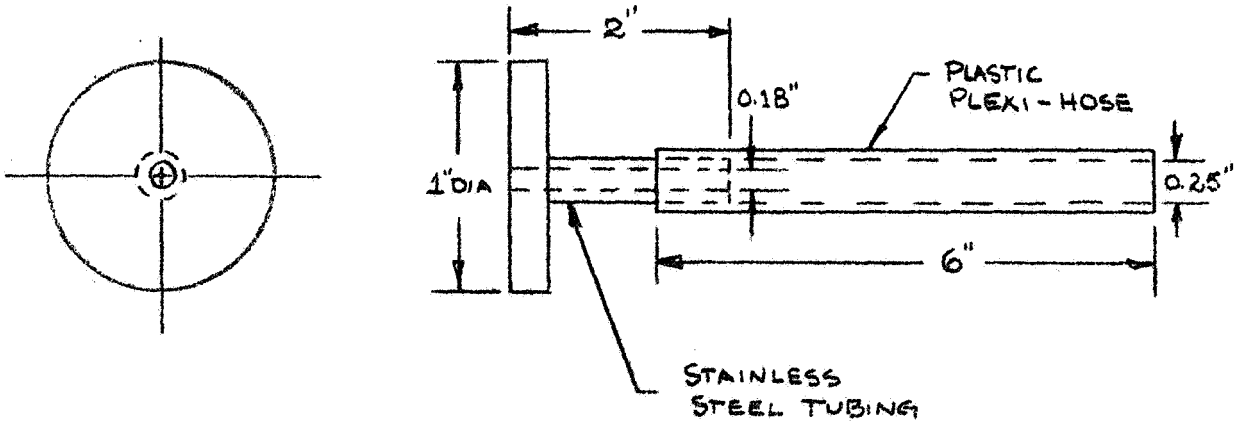

FIGURE 3b
Insert #4 Schematic

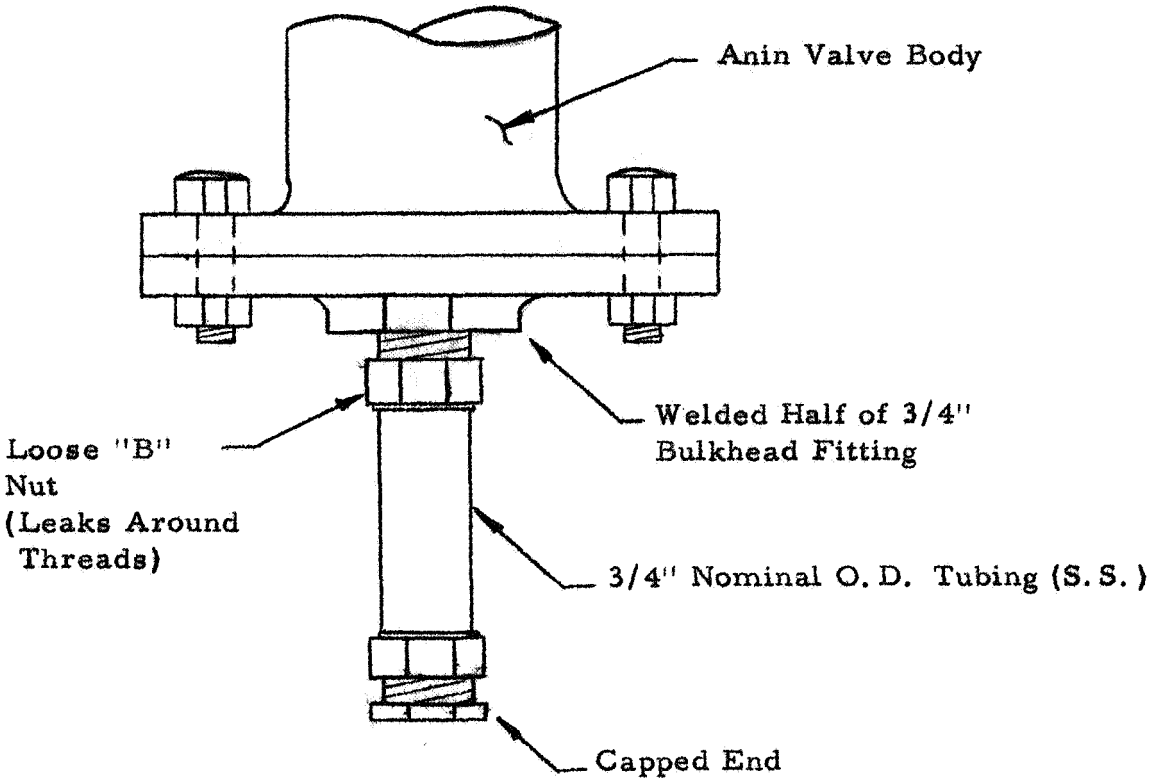

FIGURE 4a
Line Leakage Situation

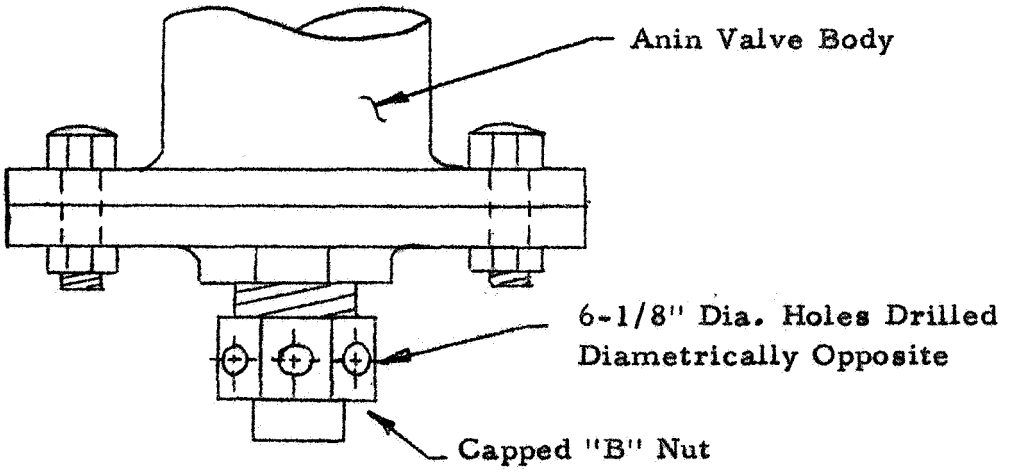

FIGURE 4b
Non-Propulsive Vent Mockup Schematic

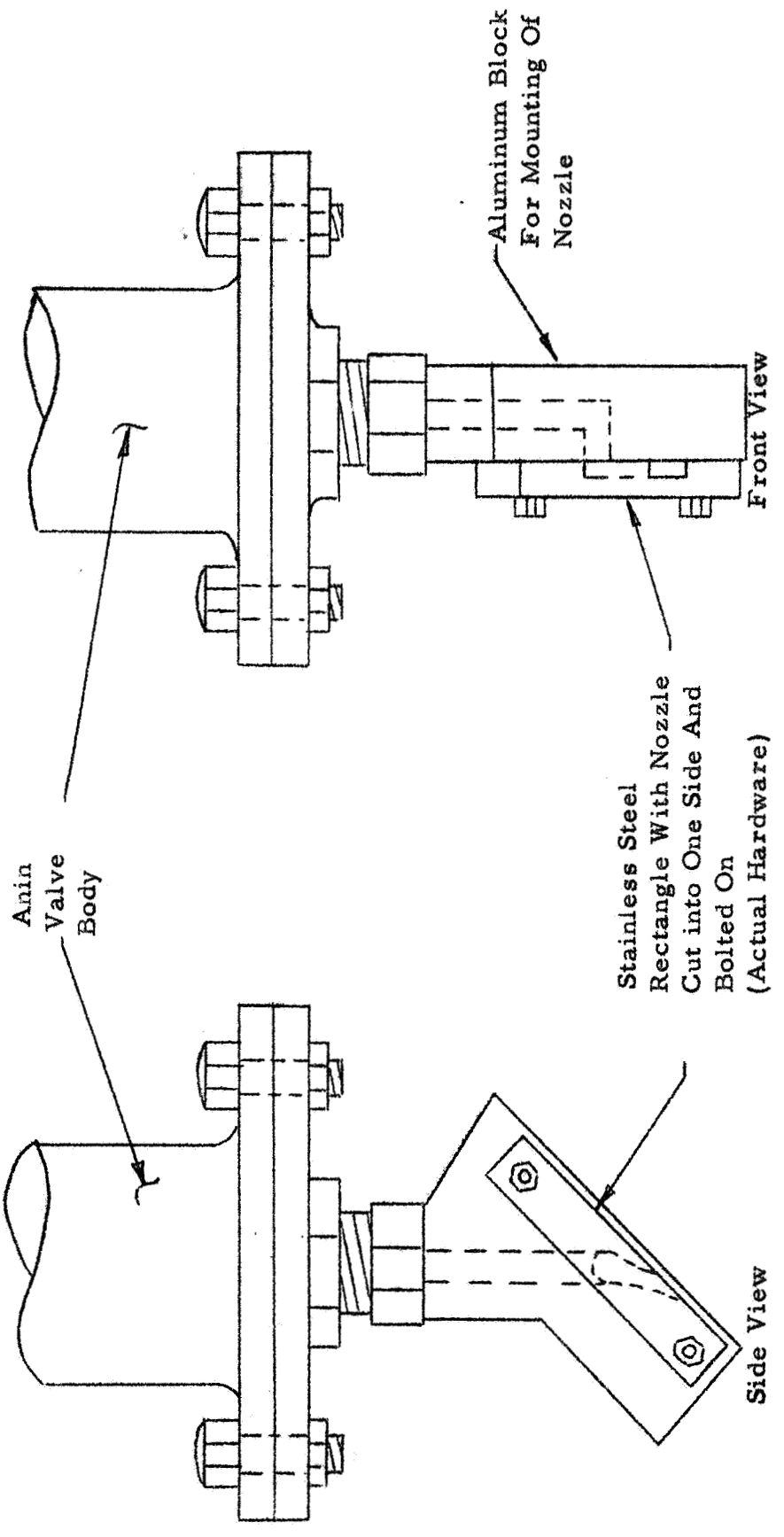

FIGURE 4C
GD/A "Zero-G" Separator Nozzle Test Fixture Schematic

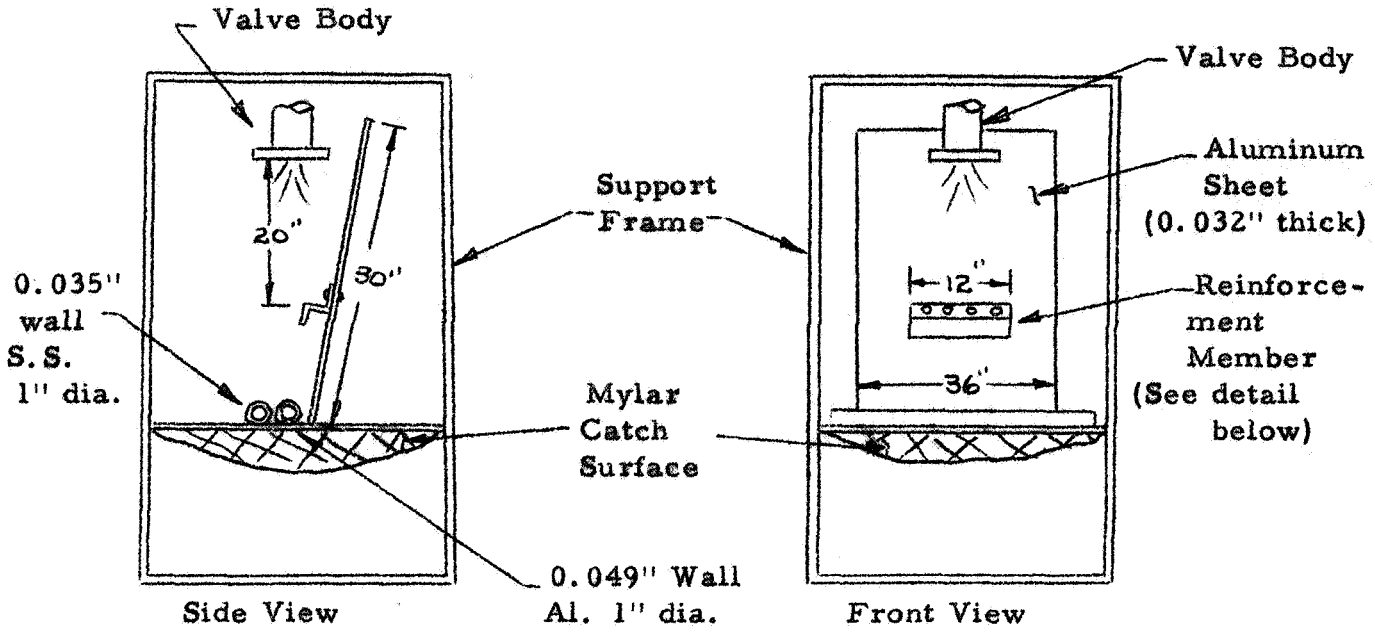

FIGURE 5a
Adapter Mockup

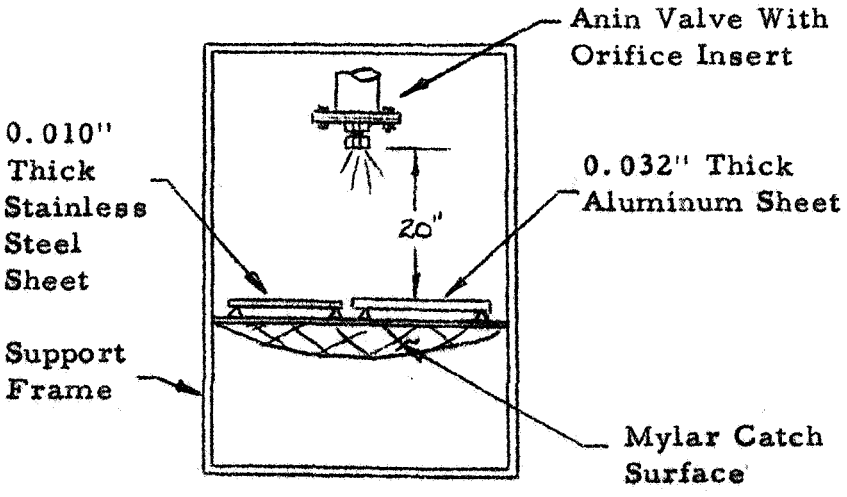

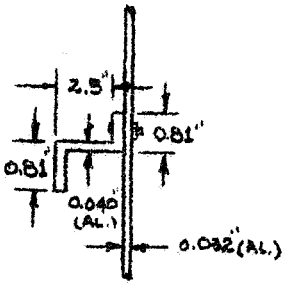

Detail of Reinforcement Member

Figure 5b
Adhesion Test Schematic

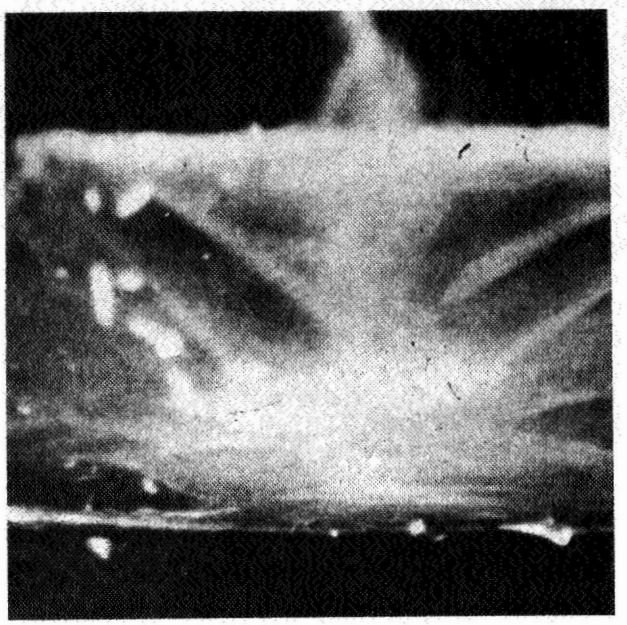

FIGURE 7
Solid Buildup on Mylar Surface From The Spray From 1" Valve Exit
(24 fr/sec)

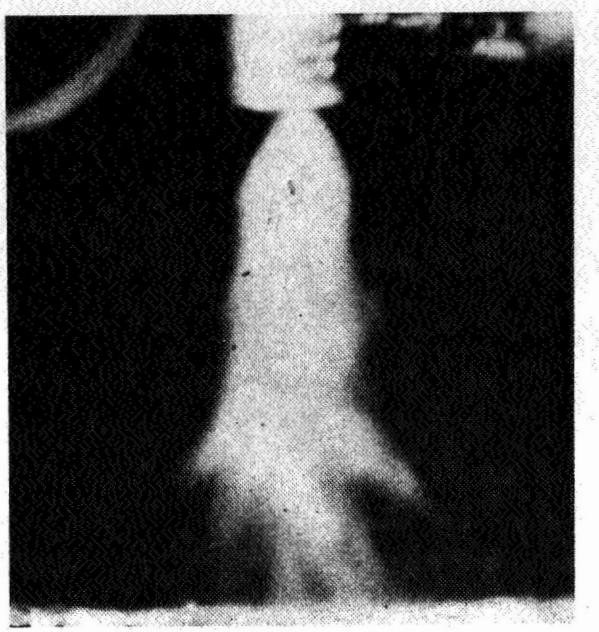

FIGURE 6
Solid Spray From 1 Inch Valve Exit
(24 fr/sec)

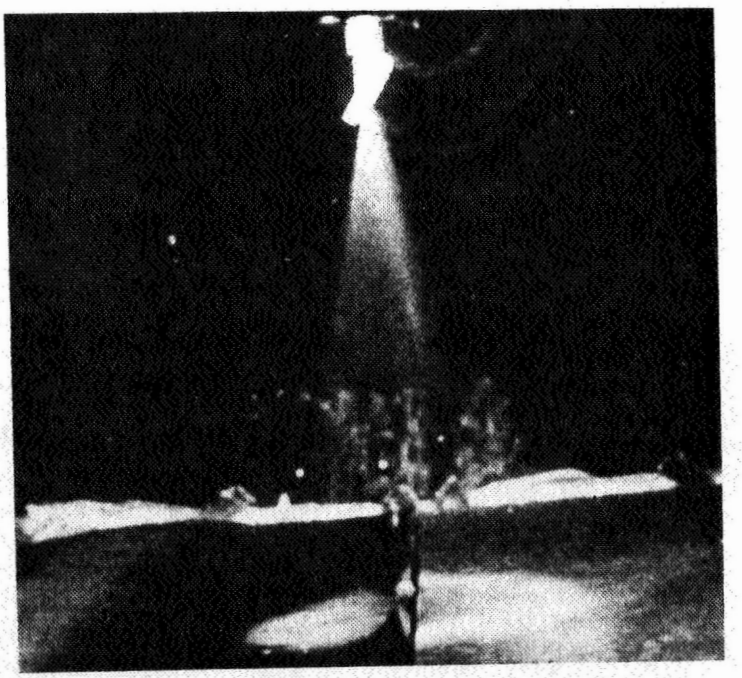

FIGURE 8
Nozzle For GD/A "Zero-g" Separator
(24 fr/sec)

III. MICRO-METEORITE PUNCTURE LEAKAGE TESTS

Because the missions of the Centaur vehicle require that it operate for prolonged periods of time in space, there is a high probability of puncture of the fuel tank skin, because of its large exposed area, by hypervelocity meteorite particles. Recovered sections of an Atlas missile have shown impacts and penetrations of the LOX tank skin by high-speed particles (References 1, 6, 7). In view of this, it is desirable to be able to accurately predict the fuel losses associated with punctures of thin gauge material (0.010" thick S.S.) by high-velocity particles in a low pressure environment. Statistical analyses by General Dynamics/Astronautics (GD/A) of the meteroid hazard to the Centaur vehicle (References 2, 3, and 4), using the available data on the meteorite flux (velocity, mass, and spacial distribution), have predicted the range of penetration area for a single puncture as 1.38×10^{-6} to 0.42 in^2, with the average puncture area of 4.18×10^{-3} in^2. This is equivalent to a circular hole with diameter ranges of 0.001 in. to 0.732 in., with an average diameter of 0.023 in. There is some question as to the relationship between meteorite particle size and velocity, the puncture area produced in a given thickness material, and the smallest mass which will penetrate a given thickness. In fact, there is a great deal of uncertainty in all areas associated with the meteorite problem. The most uncertainty, however, is associated with the meteorite flux.

The Materials Research Group at GD/A is conducting an extensive research program on hypervelocity impact on thin gauge materials both pressurized and unpressurized, Reference 5, and has produced for the author a range of sizes of hypervelocity punctures in 0.010" thick stainless steel for this study. The particle velocity was between 8,000 and 10,000 ft/sec. of 4130 steel, 0.020" dia. pellets. Photomicrographs of these holes are shown in Figures 11(a) through 11(d). Drilled holes of similar sizes are shown in Figures 11(e) and 11(f). Cross sectional views of a drilled hole and a hypervelocity puncture are shown in Figures 11(g) and 11(h).

In order to be able to more accurately predict the fuel losses on Centaur missions due to meteorite punctures, the block of tests described below were performed.

A. Test Objectives

1. Determine the flow rate and the coefficient of discharge associated with incompressible ideal fluid flow for simulated hypervelocity punctures of the Centaur fuel tank (0.010" thick stainless steel) for hole size ranging from approximately 0.001" diameter to 0.050" diameter. Testing of significantly larger holes was considered unnecessary since they would either result in catastrophic failure or excessive fuel losses.

The freezing phenomenon associated with larger holes has been tested in a previous test block, See Section II.

2. To evaluate the freezing phenomenon associated with these small holes and to determine if the holes will be plugged by the formation of solid.

B. Test Apparatus

The apparatus was arranged as shown in Figures 8(a), 8(b), 8(c) and 8(d) and consisted of the following:

1. The Aerophysics Laboratory Altitude Chamber which is capable of approximately 85 statute mile altitude pressure simulation (1×10^{-5}mmHg); it is not capable of thermal altitude simulation.
2. A pyrex and stainless steel dewar (details of construction and development program are given in the Appendix), which is structurally capable of 100 psig internal pressure. Inserts of simulated punctures were attached to the bottom flange, as shown in Figure 10. It was insulated to reduce heat input and had a transparent section, except at the flanges, so that the liquid head above the puncture could be observed.
3. A constant strength 4130 alloy steel, heat treated load beam, capable of supporting approximately a 100-lb load and deflecting (linearly) approximately 3/8" for a change in load of 2 lbs. The total mass of liquid hydrogen when the dewar was

full was approximately 2 lbs. Yield stress = 115,000 psi and Rockwell hardness = 30.

4. Cresent one-inch deflection linear transducer with resistance network and Mosley Recorder. The system was calibrated for change in weight, versus displacement. The recorder gave displacement versus time, the net result being flow rate. The accuracy of the system was a function of the calibration of the recorder and the hysteresis of the load beam.
5. One-half inch bellows type flex-hoses and stainless steel transfer lines.
6. Required valving (Jamesbury - 1/4 turn cryogenic valves) and pressure gauges.

C. Scope of Testing

The following simulated puncture holes or configurations were tested:

Specimen No.	Hole Size (approx.) (in) Impact Side	Reverse Side	Type of Hole	Sheet Material	Sheet Thickness (in)	Figure Number	Fluid Used
1	0.020	0.004 x 0.010	hyper-velocity	S. S.	0.010	11(a)	LH_2
2	0.027	0.027	hyper-velocity	S. S.	0.010	11(b)	LH_2
3	0.020	0.020	hyper-velocity	S. S.	0.010	11(c)	LH_2
4	0.013	0.004	hyper-velocity	S. S.	0.010	11(d)	LH_2 & LN_2
5	0.014	0.014	drilled (#80 drill)	S. S.	0.010	11(e)	LH_2
6	0.048	0.048	drilled (#56 drill)	S. S.	0.010	11(f)	LH_2
7	0.014	0.014	drilled (#80 drill)	plexi-glass	0.375	11(j)	LN_2

Figures 11(a) thru 11(f) were enlarged 24 times actual size. Impact velocity was between 8,000 and 10,000 ft/sec for punctures shown in Figures 11(c) thru 11(f).

D. Test Results

The experimental measurements of the flow rate and subsequent calculations of the coefficient of discharge associated with incompressible ideal fluid flow for the various hole sizes tested are shown in Table 1. The coefficient of discharge is plotted as a function of approximate hole diameter in Figure 12. An analysis of Table I and Figure 12 shows a considerable scatter in the results for a single hole. Errors could have been introduced from the following sources:

(1) Inaccuracies of the measuring system caused by hysteresis of the load beam, the calibration range of the recorder, and the non-linearity of output from the transducer. When the system was calibrated for full-scale recorder reading for a change in load of 800 grams (approximately 2.0 lbs), the accuracy was approximately 50-60%. For a similar full scale reading for 400 grams, the accuracy was about 25-30%.

(2) The variations of the jet thrust of the fluid escaping through the hole with changes in dewar internal pressure. The change in magnitude of the thrust was approximately the same order of magnitude as the mass flow rate when the change in the dewar internal pressure was about

MICRO-METEORITE PUNCTURE LEAKAGE STUDY

Test Results 4/25/62 to 6/18/62

Test No:	Date Tested	Specimen No.	Hole Impact Side (in. dia)	Size Reverse Side (in. dia)	Thickness of Base Mat'l (in)	Min. Area (ft^2) x 10^7	Hole Type	Average Ullage Pressure (psia)	Average Saturated Liquid Density (lb/ft^3)	Calculated Flow Rate* (lb/sec) x 10^{+4}	Measured Flow Rate (grams/min)	Measured Flow Rate (lb/sec) x 10^4	Coefficient of Discharge	Movie Reel No.	Film Speed Frames/Sec	Full Scale Calibration (Grams)	COMMENTS
1(a)	4/25/62	5	0.014	0.014	0.010	9.94	Drilled	34.5	4.15	11.4	13.6	5.0	0.44	2-color	24	800	Pellets of solid about hole size
1(b)	4/25/62	5	0.014	0.014	0.010	9.94	Drilled	39.5	4.10	12.2	6.7	2.47	0.20	2-color	24	800	form & come out in a cone
3(a)	5/4/62	5	0.014	0.014	0.010	9.94	Drilled	42.0	4.08	12.6	16.3	5.98	0.48	2-color	24	800	shaped shower.
3(b)	5/4/62	5	0.014	0.014	0.010	9.94	Drilled	39.5	4.10	12.2	22.5	8.26	0.68	2-color	24	800	
3(c)	5/4/62	5	0.014	0.014	0.010	9.94	Drilled	34.5	4.13	11.4	6.7	2.47	0.22	2-color	24	800	
3(d)	5/4/62	5	0.014	0.014	0.010	9.94	Drilled	34.5	4.13	11.4	7.2	2.65	0.23	2-color	24	800	
3(e)	5/4/62	5	0.014	0.014	0.010	9.94	Drilled	15.5	4.40	7.9	5.3	1.94	0.25	2-color	24	800	
3(f)	5/4/62	5	0.014	0.014	0.010	9.94	Drilled	39.5	4.10	12.2	4.6	1.70	0.14	2-color	24	800	
3(g)	5/4/62	5	0.014	0.014	0.010	9.94	Drilled	39.5	4.10	12.2	4.3	1.56	0.13	2-color	24	800	
4(a)	6/5/62	5	0.014	0.014	0.010	9.94	Drilled	34.5	4.13	11.4	13.3	4.9	0.43	3-B&W	128	800	Pellets form by building up and
4(b)	6/5/62	5	0.014	0.014	0.010	9.94	Drilled	39.5	4.10	12.2	13.3	4.9	0.40	3-B&W	128	800	blowing out.
4(c)	6/5/62	5	0.014	0.014	0.010	9.94	Drilled	32.0	4.18	11.1	7.7	2.8	0.26	3-B&W	128	800	
4(d)	6/5/62	5	0.014	0.014	0.010	9.94	Drilled	39.5	4.10	12.2	7.9	2.8	0.25	3-B&W	128	800	
5(a)	6/7/62	6	0.048	0.048	0.010	121.0	Drilled	29.5	4.22	110.	160	59	0.54	4-B&W	128	800	Cone Shaped Mist of minute
5(b)	6/7/62	6	0.048	0.048	0.010	121.0	Drilled	39.5	4.10	147.5	229	84	0.57	4-B&W	128	800	particles.
5(c)	6/7/62	6	0.048	0.048	0.010	121.0	Drilled	39.5	4.10	147.5	220	81	0.55	4-B&W	128	800	
6(a)	6/15/62	1	0.020	0.004 x 0.010	0.010	4.8	Hyper-velocity	29.5	4.22	5.15	3.7	1.36	0.27	5-B&W	128	800	Pellets about hole size were
6(b)	6/15/62	1	0.020	"	0.010	4.8	" "	29.5	4.22	5.15	3.6	1.34	0.26	5-B&W	128	800	formed.
6(c)	6/15/62	1	0.020	"	0.010	4.8	" "	27.0	4.24	4.94	5.6	2.04	0.41	5-B&W	128	800	
6(d)	6/15/62	1	0.020	"	0.010	4.8	" "	34.5	4.13	5.52	3.6	1.30	0.24	5-B&W	128	800	
7(a)	6/18/62	1	0.020	0.004 x 0.010	0.010	4.8	Hyper-velocity	32.0	4.18	5.35	6.3	2.3	0.43	6-B&W	400	400	Tiny Pellets about hole size
7(b)	6/18/62	1	0.020	" "	0.010	4.8	" "	29.5	4.22	5.14	9.4	3.5	0.67	6-B&W	400	400	are formed.
7(c)	6/18/62	1	0.020	" "	0.010	4.8	" "	21.5	4.31	4.45	2.3	0.8	0.18	6-B&W	400	400	
7(d)	6/18/62	1	0.020	" "	0.010	4.8	" "	21.5	4.31	4.45	2.8	1.0	0.23	6-B&W	400	400	
7(e)	6/18/62	1	0.020	" "	0.010	4.8	" "	21.5	4.31	4.45	2.9	1.1	0.24	6-B&W	400	400	
7(f)	6/18/62	1	0.020	" "	0.010	4.8	" "	19.5	4.34	4.23	3.6	1.3	0.32	6-B&W	400	400	
7(g)	6/18/62	1	0.020	" "	0.010	4.8	" "	19.5	4.34	4.23	4.1	1.5	0.36	6-B&W	400	400	
8	6/18/62	1	0.020	0.004 x 0.010	0.010	4.8	Hyper-velocity	19.5	4.34	4.23	4.1	1.5	0.36	7-B&W	400	400	

* $w = A\sqrt{2g_c \rho \Delta P}$

MICRO-METEORITE PUNCTURE LEAKAGE STUDY.

Test Results 9/11/62 to 2/6/63

Test No.	Date Tested	Specimen No.	Hole Size Impact Side (in)	Hole Size Reverse Side (in)	Thickness of Base Mat'l (in)	Min. Area (ft^2) x 10^7	Hole Type	Ave. Ullage Press. (psia)	Ave. Sat. Liquid Density (lb/ft^3)	Calculated Flow Rate* (lb/sec) x 10^4	Measured Flow Rate (grams/min)	Measured Flow Rate (lb/sec) x 10^4	Coefficient of Discharge $C_o = \frac{W_M}{W_{cal}}$	Movie Reel No.	Film Speed (frames/sec)	Full Scale Calib. (grams)	COMMENTS
9(a)	9/11/62	3	0.020	0.020	0.010	20.8	Hyper-velocity	34.5	4.13	24.0	20	7.4	0.30	8-B&W	400	500	Small pellets formed
9(b)	9/11/62	3	0.020	0.020	0.010	20.8	" "	24.5	4.27	20.2	10	3.7	0.19	9-B&W	400	500	about periphery and
9(c)	9/11/62	3	0.020	0.020	0.010	20.8	" "	54.5	3.90	29.2	9	3.3	0.12	10-B&W	400	500	spray mist in the center.
9(d)	9/11/62	3	0.020	0.020	0.010	20.8	" "	22.0	4.30	19.7	9.3	3.4	0.17	11-B&W	400	500	
9(e)	9/11/62	3	0.020	0.020	0.010	20.8	" "	27.0	4.24	21.4	10.5	3.9	0.18	11-B&W	400	500	
9(f)	9/11/62	3	0.020	0.020	0.010	20.8	" "	24.5	4.27	20.2	7.2	2.7	0.14	11-B&W	400	500	
10(a)	9/21/62	3	0.020	0.020	0.010	20.8	Hyper-velocity	27.0	4.25	21.3	55.6	20.4	0.96	12-B&W	1300	300	The lower seal was
10(b)	9/21/62	3	0.020	0.020	0.010	20.8	" "	27.0	4.25	21.3	71.0	26.2	1.23	13-B&W	1300	300	leaking - the results
10(c)	9/21/62	3	0.020	0.020	0.010	20.8	" "	27.0	4.25	21.3	67.7	24.9	1.16	14-B&W	1300	300	are very questionable.
10(d)	9/21/62	3	0.020	0.020	0.010	20.8	" "	24.5	4.28	20.4	45.2	16.6	0.82	15-B&W	1300	300	
10(e)	9/21/62	3	0.020	0.020	0.010	20.8	" "	24.5	4.28	20.4	44.3	16.3	0.80	15-B&W	1300	300	
11(a)	9/24/62	4	0.013	0.004	0.010	1.04	Hyper-velocity	29.5	4.22	1.11	4.3	1.58	1.4	16-B&W	1300	300	Results are questionable
11(b)	9/24/62	4	0.013	0.004	0.010	1.04	" "	29.5	4.22	1.11	4.5	1.64	1.5	16-B&W	1300	300	because of extremely
11(c)	9/24/62	4	0.013	0.004	0.010	1.04	" "	24.5	4.28	1.03	2.2	0.82	0.8	17Color	1000	300	small flow-plugged until
11(d)	9/24/62	4	0.013	0.004	0.010	1.04	" "	24.5	4.28	1.03	0.8	0.30	0.29	17Color	1000	300	about 30 psid across
11(e)	9/24/62	4	0.013	0.004	0.010	1.04	" "	24.5	4.28	1.03	0.4	0.15	0.15	18-B&W	1300	300	hole.
11(f)	9/24/62	4	0.013	0.004	0.010	1.04	" "	52.0	3.98	1.44	2.0	0.74	0.52	18-B&W	1300	300	
11(g)	9/24/62	4	0.013	0.004	0.010	1.04	" "	37.0	4.13	1.23	1.4	0.51	0.41	18-B&W	1300	300	
12(a)	9/28/62	7	0.014	0.014	0.375	9.94	Drilled	30	Did not measure flow rate - mat'l - plexi-glass -					19-B&W	400 -6"	lens	Film was no good.
12(b)	9/28/62	7	0.014	0.014	0.375	9.94	Drilled	30	attempted to photograph liquid - solid interface					20-B&W	400/128	"	Pellets form in tiny hole.
12(c)	9/28/62	7	0.014	0.014	0.375	9.94	Drilled	30	or freezing phenomena.					21-B&W	400/128	2" lens	Plexi-glass dewar cracked
12(d)	9/28/62	7	0.014	0.014	0.375	9.94	Drilled	30						22-B&W	400		due to thermal stresses-
12(e)	9/28/62	7	0.014	0.014	0.375	9.94	Drilled	30						23-B&W	128		leaked badly & extruded
																	large chunks of solid N_2.
15(a)	2/6/63	2	0.027	0.027	0.010	42.2	Hyper-velocity	37	4.125	50.2	11.75	4.33	0.09			400	Both solid pellets and
15(b)	2/6/63	2	0.027	0.027	0.010	42.2	" "	37	4.125	50.2	14.5	5.34	0.11			400	spray mist were
15(c)	2/6/63	2	0.027	0.027	0.010	42.2	" "	37	4.125	50.2	13.75	5.06	0.10			400	produced.
15(d)	2/6/63	2	0.027	0.027	0.010	42.2	" "	37	4.125	50.2	10.3	3.8	0.08			400	

* $w = A\sqrt{2g_c \bar{\rho} \Delta P}$

75-100 psid. The thrust was calculated assuming ideal incompressible flow.

(3) The effect of liquid hydrogen temperature on the calibration and the resistance to vertical motion of the dewar offered by the attached fill and vent lines. The system was calibrated at atmospheric conditions and, under these conditions, the restraints offered negligible resistance when pressurized or unpressurized.

(4) Small particles of foreign material in the liquid. In the test with the 0.027" diameter hole, small particles were observed in the dewar after the test.

(5) The surface roughness of the holes which could cause solid hydrogen to accumulate at various points around the perimeter of the hole and thereby varying the effective hole area for the various tests of the same hole specimen.

Based on the results shown in Table I, it is not possible to establish exact values for the coefficient of discharge for the hole sizes tested, but only to indicate approximate ones and general trends. The dotted line on Figure 12 represents what the data indicates to be the equilibrium conditions. Additional test points are needed to complete the

curve in Figure 12. However, priority needs for LH_2 prematurely terminated the tests.

Generally there is a trend for a decreasing coefficient of discharge with time and decreasing hole size. The test data in Table I is arranged in consecutive order with respect to time. This may be indicative of decreasing effective area due to solid accumulation in the hole as the fixture chills down. The later values in each test block should be more representative of the equilibrium state. On Figure 12 a dip in the coefficient of discharge is indicated in the hole size range of about 0.020" to 0.030". This could be due to increased turbulence because of the transition in flow phenomenon.

The hole size has a very definite affect on the freezing phenomenon which affects the flow rate and consequently the coefficient of discharge. For holes larger than approximately 0.020" to 0.030" diameter, the solid appeared in a mist of very minute particles and there was a continuous flow of mass (See Figure 15 for a photograph of flow from an 0.048" diameter drilled hole). For hole sizes less than about 0.020" to 0.030" diameter, the flow was no longer continuous,

but was made up of gas and small, solid pellets of approximately the same size as the hole. These pellets apparently were formed by successively building up in the hole and being blown out by the pressure difference across the hole. (See Figures 13 and 14). If the flow measuring system was sensitive enough, the recorded flow should be step functions under these conditions. The transition in flow phenomenon occured at approximately 0.020" to 0.030" diameter, where there was a combination of pellets and spray mist as shown in Figure 16. For very small holes (see test #11 in Table 1 for a 0.004" diameter hole test results), there was no visible or measurable flow by the methods used until a definite $\triangle P$ across the hole was reached. For specimen #6 this was about 30 psid. When the hole size was such that pellets were produced, the size of the particles decreased as the $\triangle P$ across the hole increased, i.e., they tended to approach the spray mist configuration associated with the larger holes.

For the very small holes the complete plugging could be maintained for any extended length of time, as was observed, if: (1) the solid end of the plug exposed to the low pressure sublimed and consequently froze more liquid on the end

immersed in liquid, or in other words, an actual mass flow was maintained; or, (2) impurities or foreign material such as H_2O or metal bits existed in the LH_2 or LN_2 which could lodge in the hole. It should be pointed out that the above discussion of the variation of flow configuration with hole size was determined only for a 0.010" thick plate. Further experiments should be conducted to determine if the same applies for thicker plates.

If the length of the hole is large for the very small holes (large L/D ratio), the flow will be in the form of intermittant solid extrusions. This is seen in Figure 16 where flow occurred through a crack in a 3/4" wall plexiglass dewar.

In all cases a coefficient of discharge of 0.6 or 0.7 appears to be conservative in estimating the fuel losses in space due to meteorite punctures. For very small holes the coefficient of discharge is lower because of the fluctuating flow due to intermittant plugging of the hole by the solid formation. For holes less than 0.020" diameter in 0.010" thick material, use of a coefficient of discharge of about 0.3 or 0.4 would be realistic.

E. Film Record

Representative sections of the film for this block of the testing has been compiled, edited, and separated with titles into a one-reel film entitled, "Micro-Meteorite Puncture Leakage Study". This is kept on file by the Motion Pictures and Television Group, Department 120-4. The originals of all the film taken in this block of testing, filed by reel number as defined in Table 1, is also kept on file by the same group under the general title of "Micro-Meteorite Study".

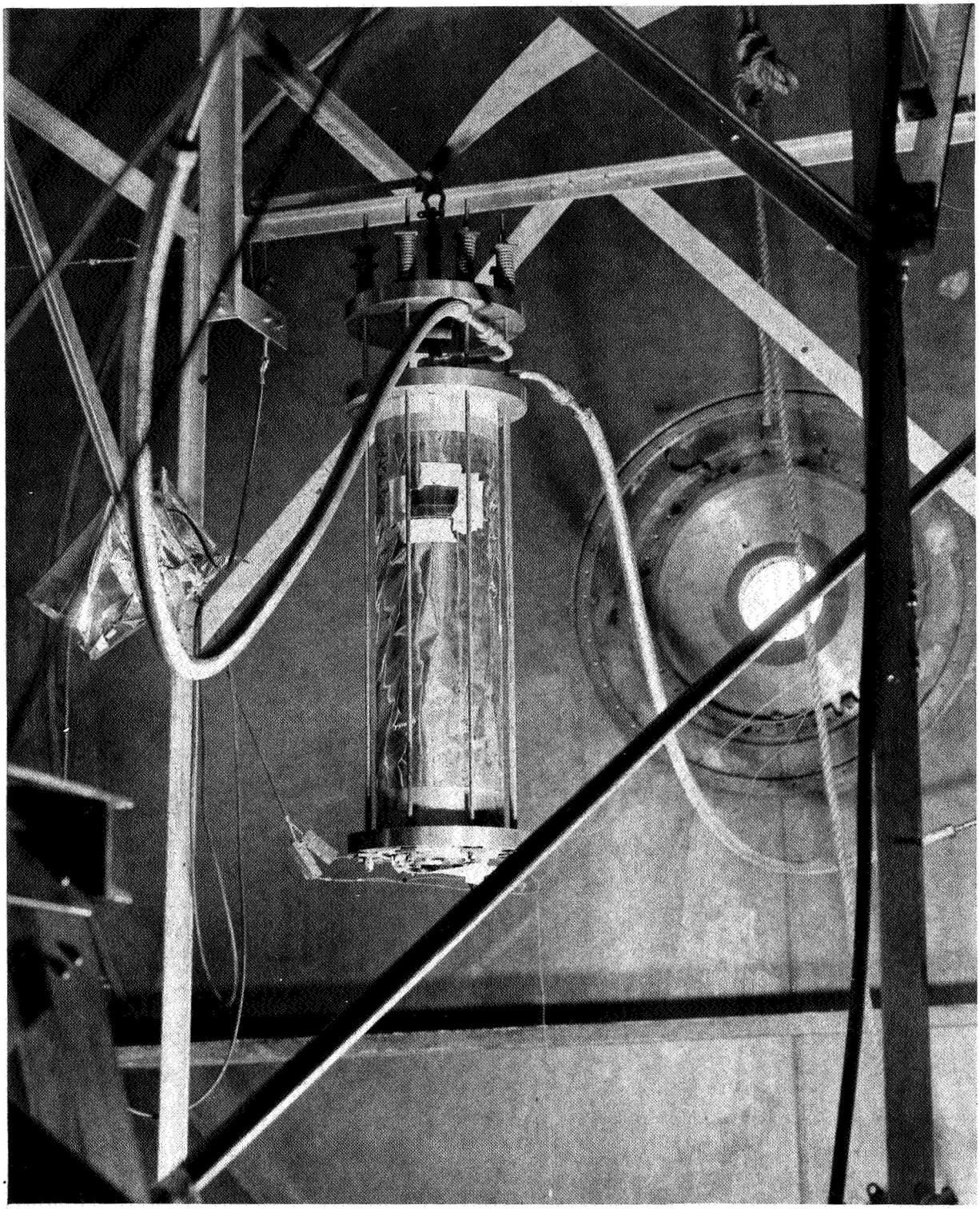

FIGURE 9(a)
Test Setup
Rear View

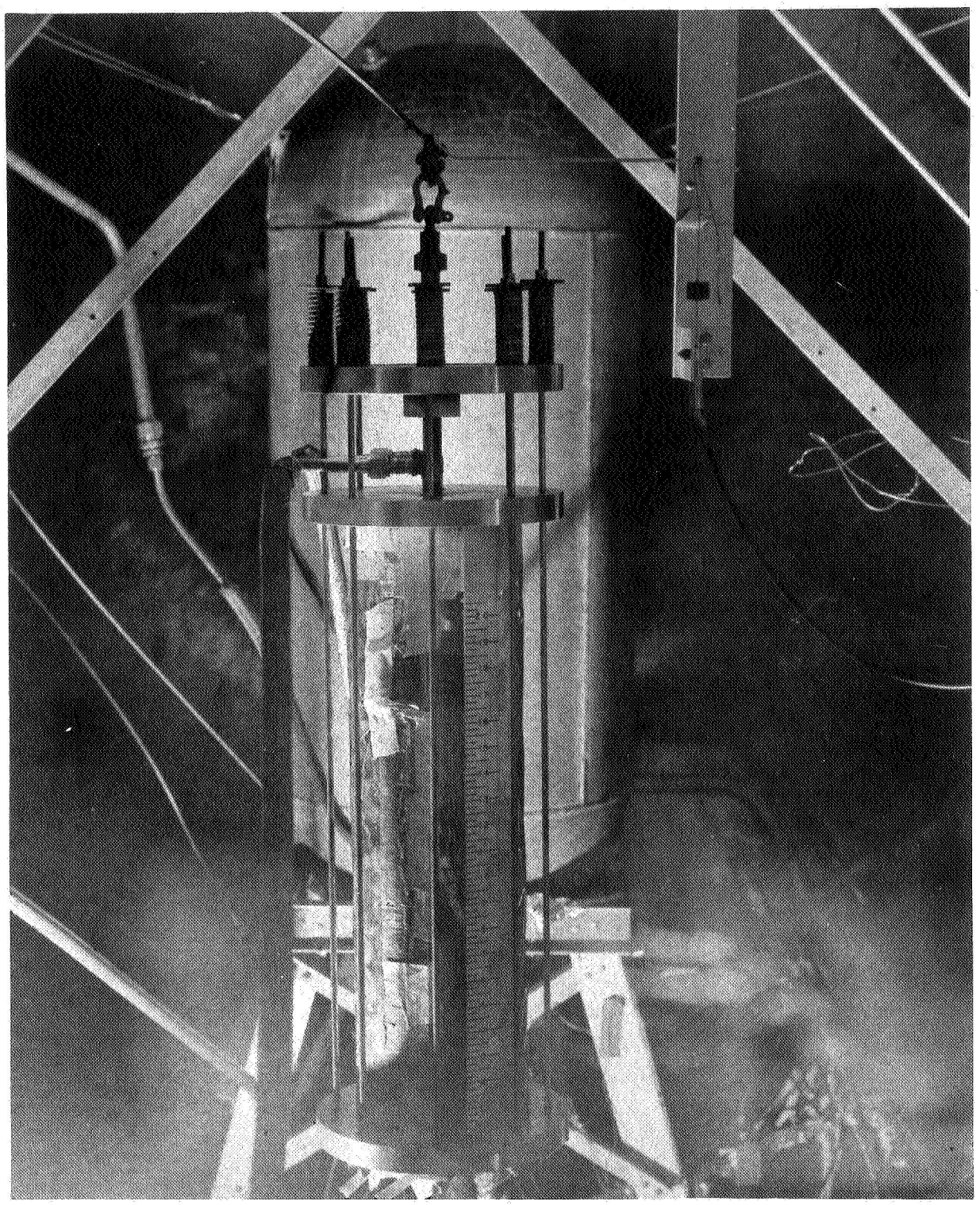

FIGURE 9(b)
Test Setup
Front View

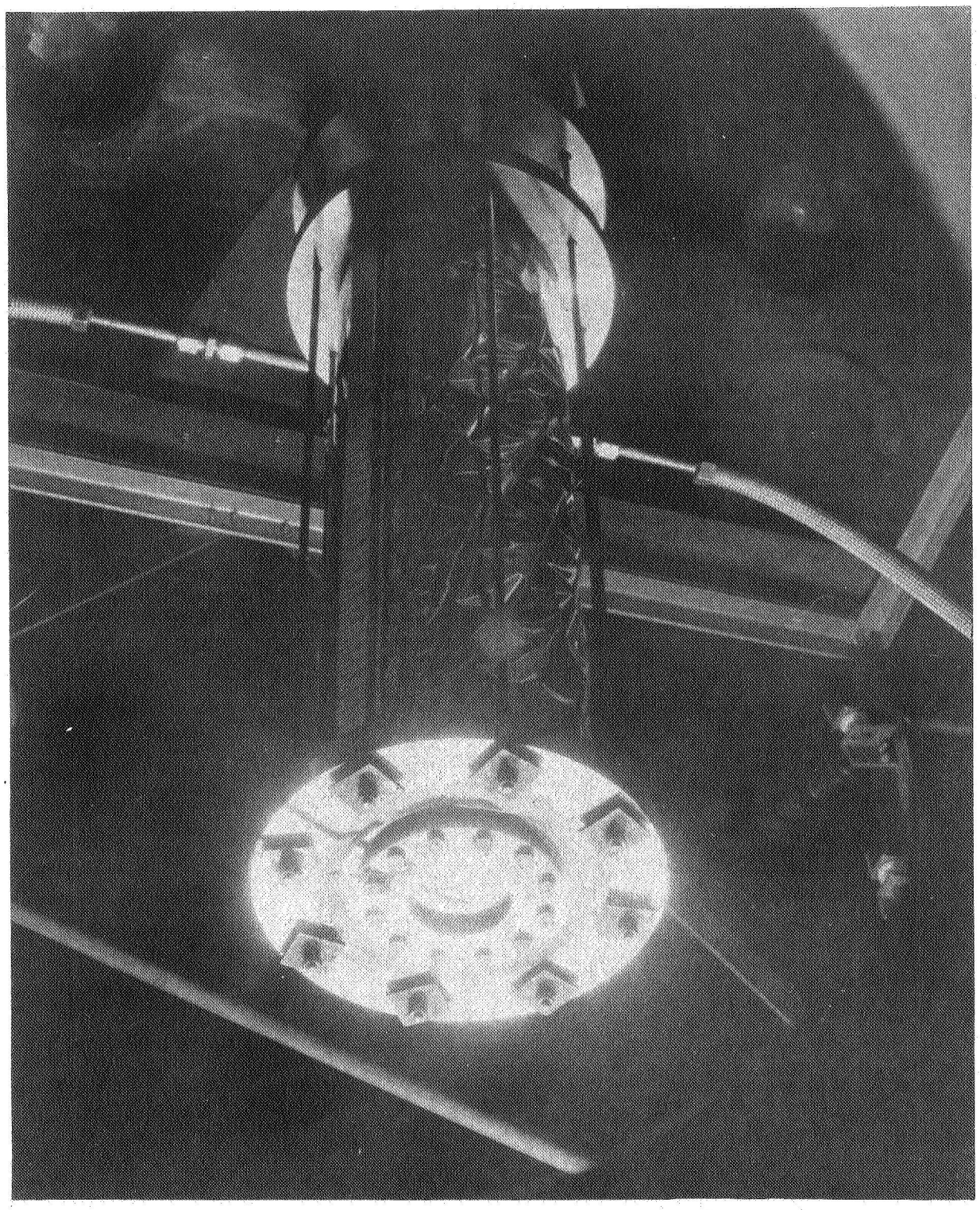

FIGURE 9(c)
Test Setup
Bottom View

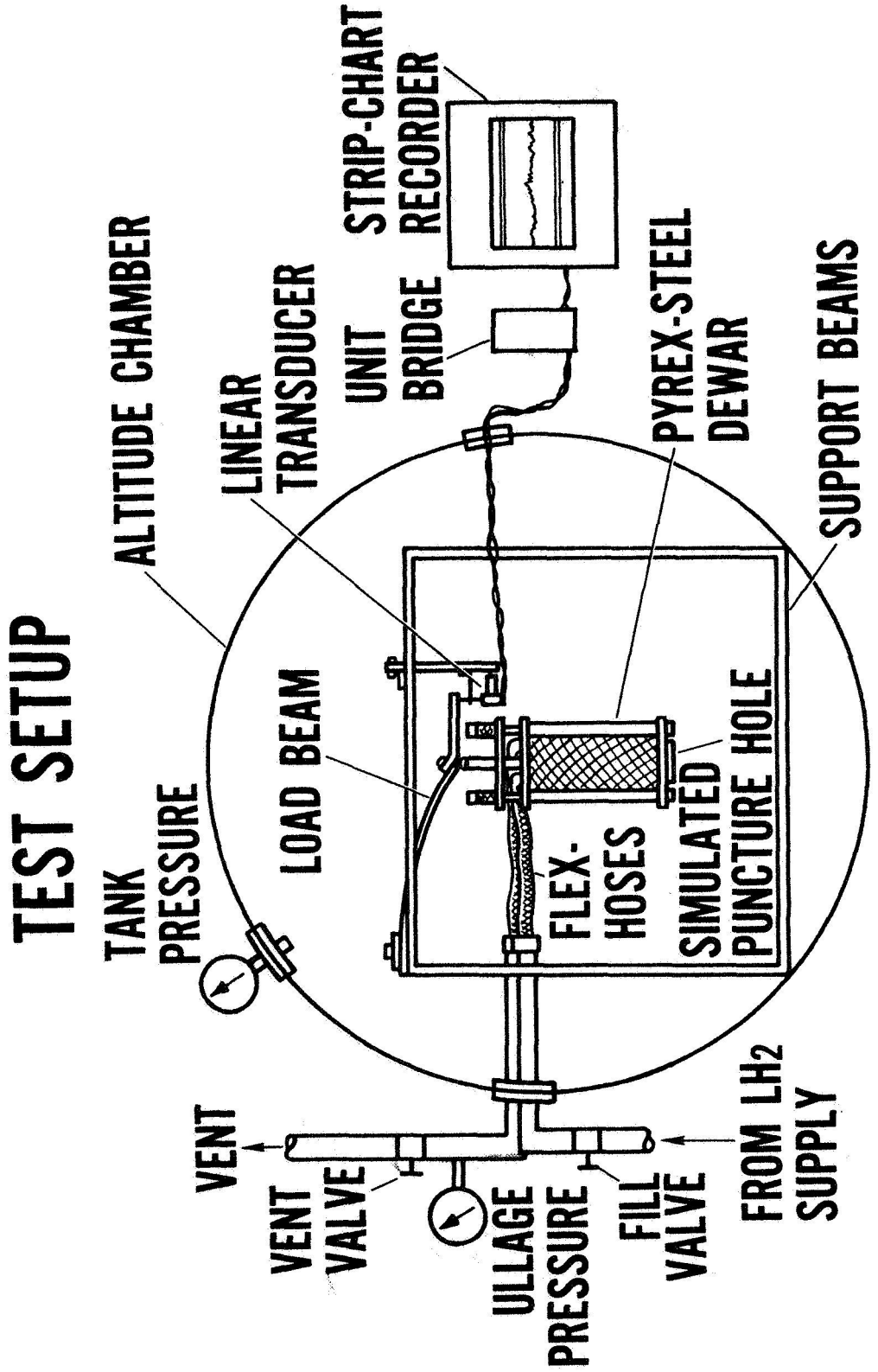

FIGURE 9d
Micro-Meteorite Puncture Leakage Study

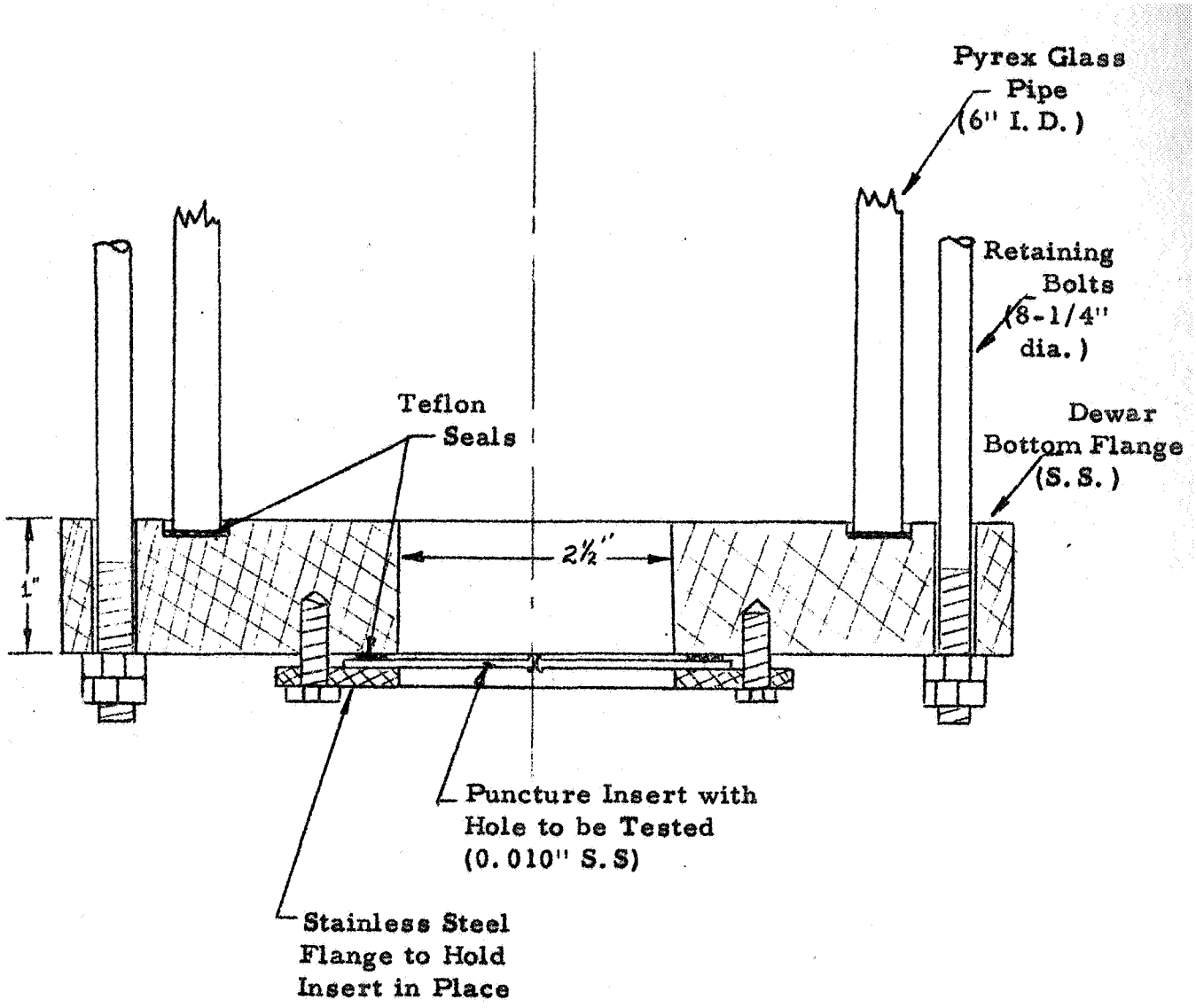

FIGURE 10
Attachment of Puncture Specimen Insert
(Crossectionally)

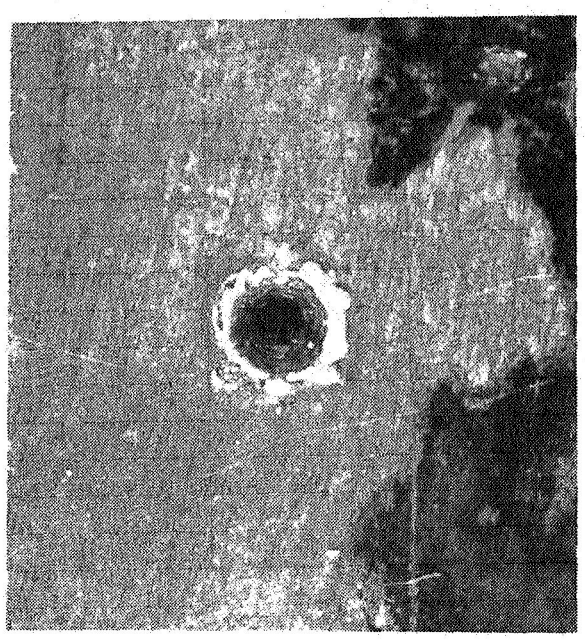

Impact Side

Reverse Side

FIGURE 11(a)
Specimen Puncture #1

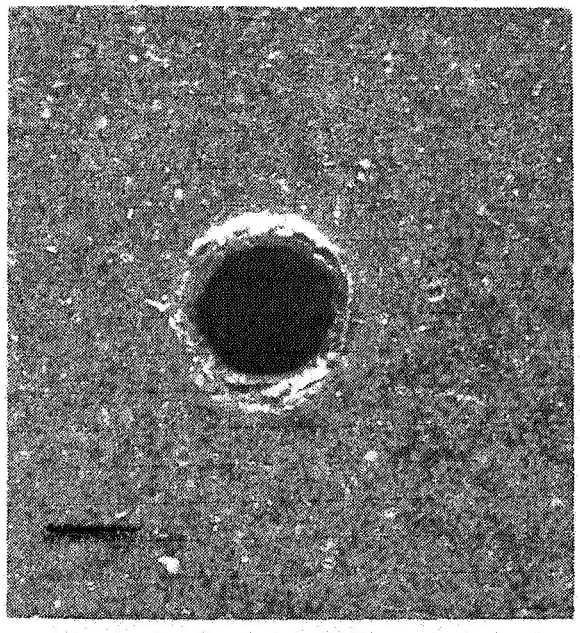

Impact Side

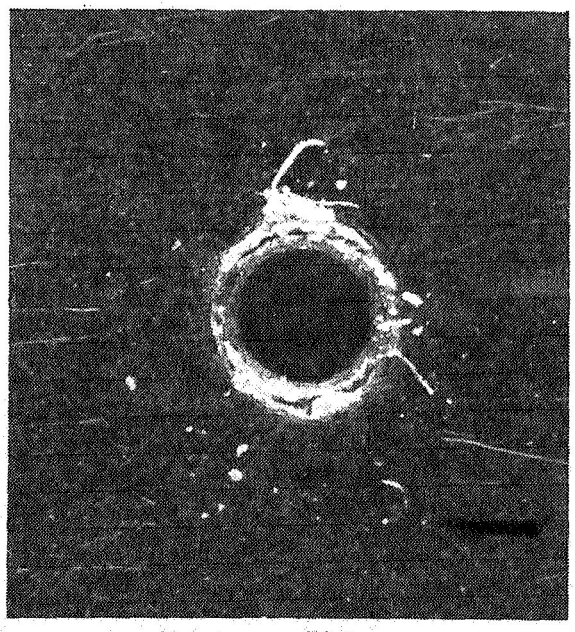

Reverse Side

FIGURE 11(b)
Specimen Puncture #2

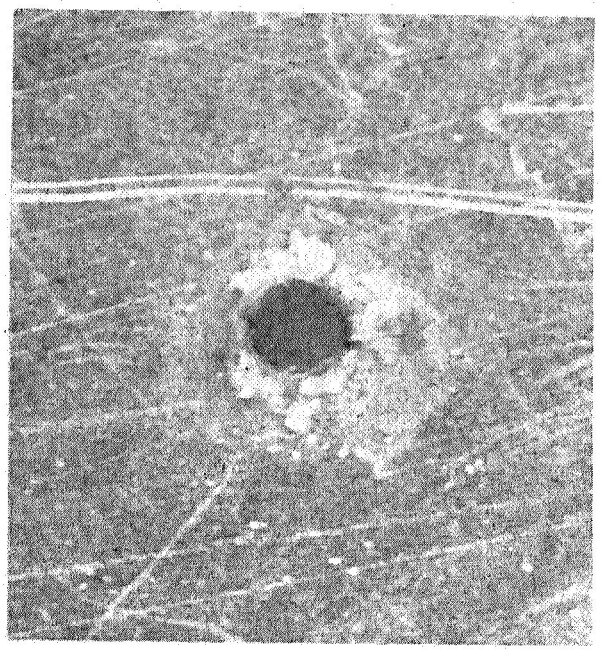

Impact Side

Reverse Side

FIGURE 11(c)
Specimen Puncture #3

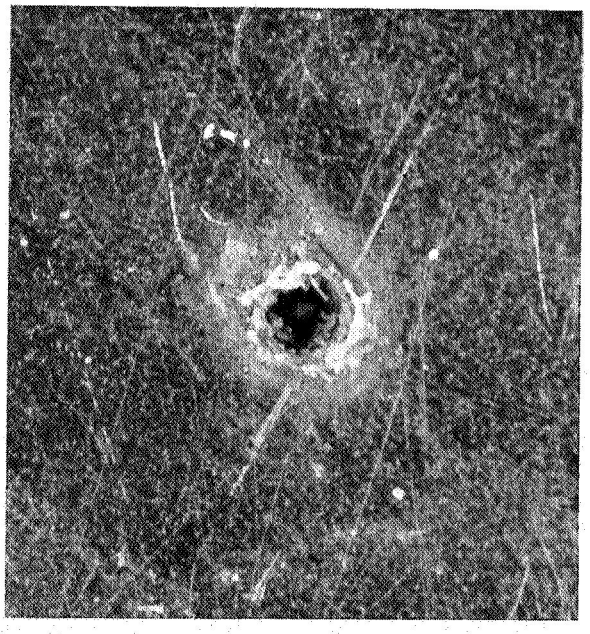

Impact Side

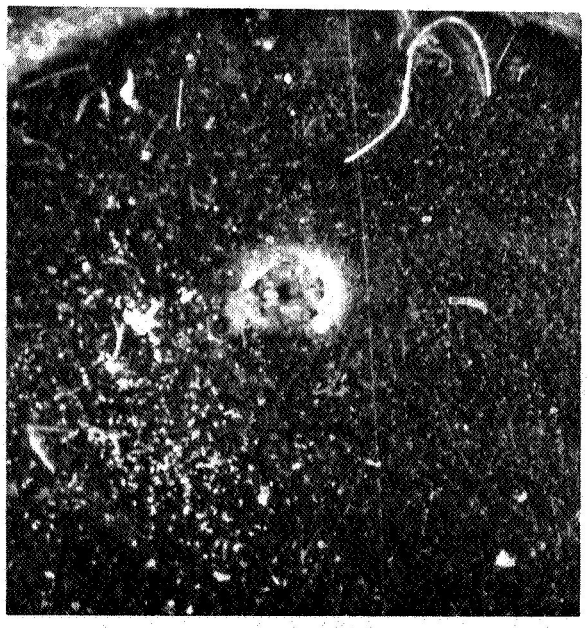

Reverse Side

FIGURE 11(d)
Specimen Puncture #4

Impact Side
(side which drill entered)

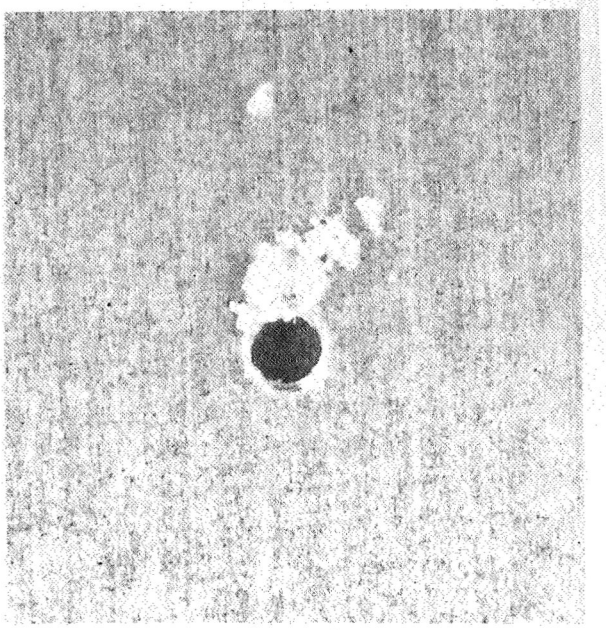

Reverse Side

FIGURE 11(e)
Specimen Puncture #5

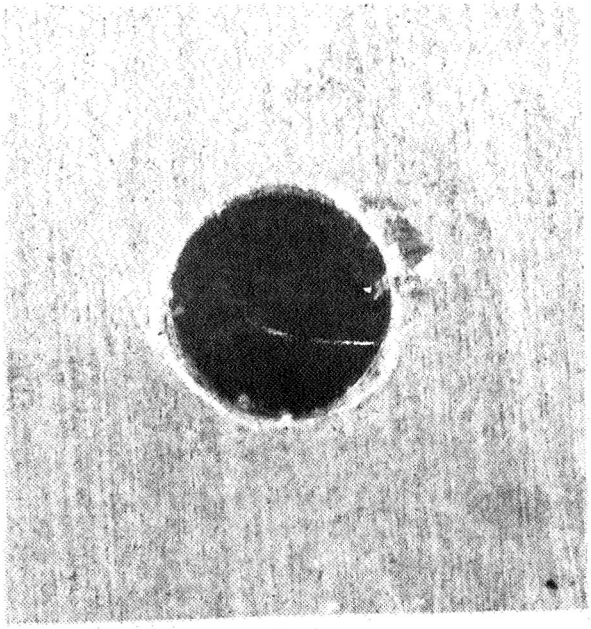

Impact Side
(side which drill entered)

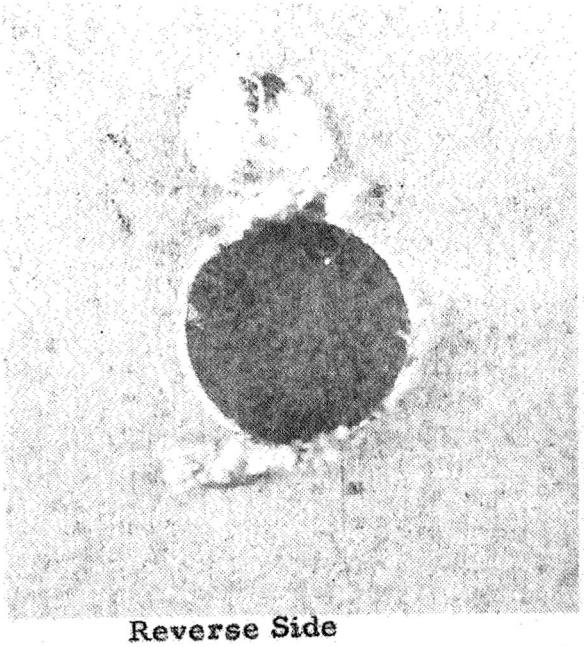

Reverse Side

FIGURE 11(f)
Specimen Puncture #6

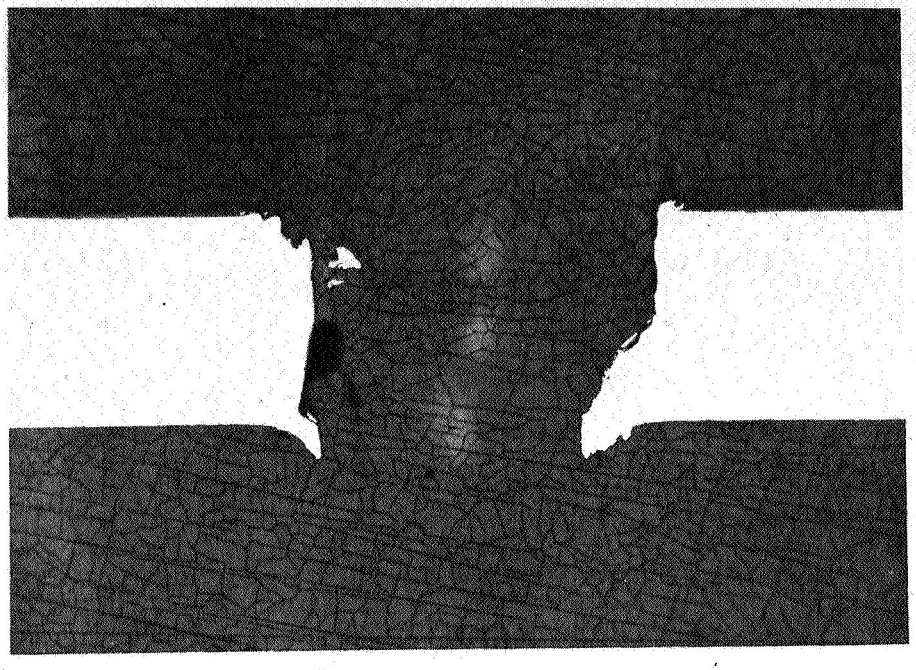

FIGURE 11(g)
Cross-Section of a Drilled Hole of Same Size as Specimen Puncture #5
(Dia = 0.014; Magification = 100X)

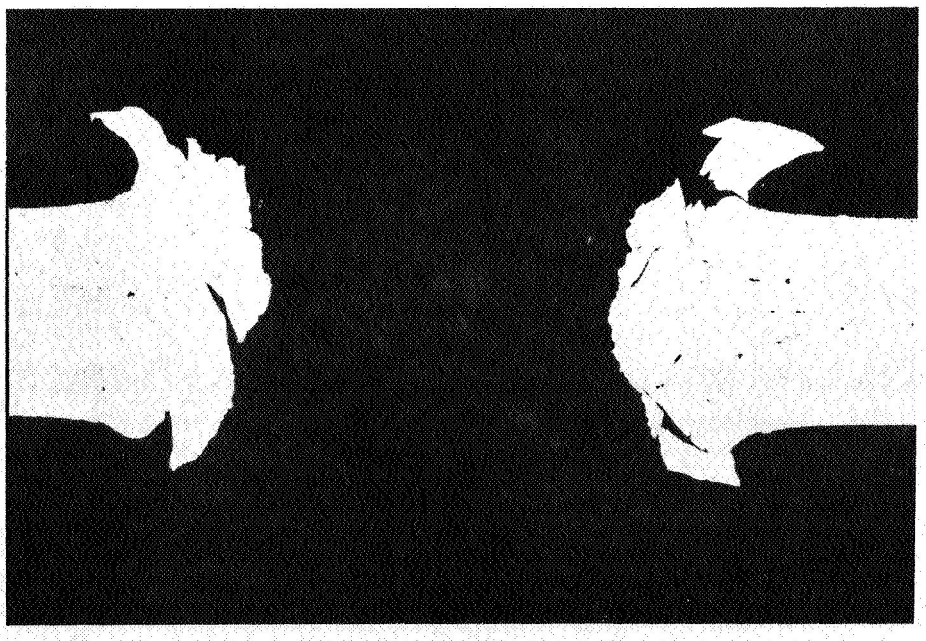

FIGURE 11(h)
Cross-Section of Hyper-Velocity Puncture
(Dia = 0.018"; Magification = 100X)
Impact Velocity ≐ 10,000 ft/sec

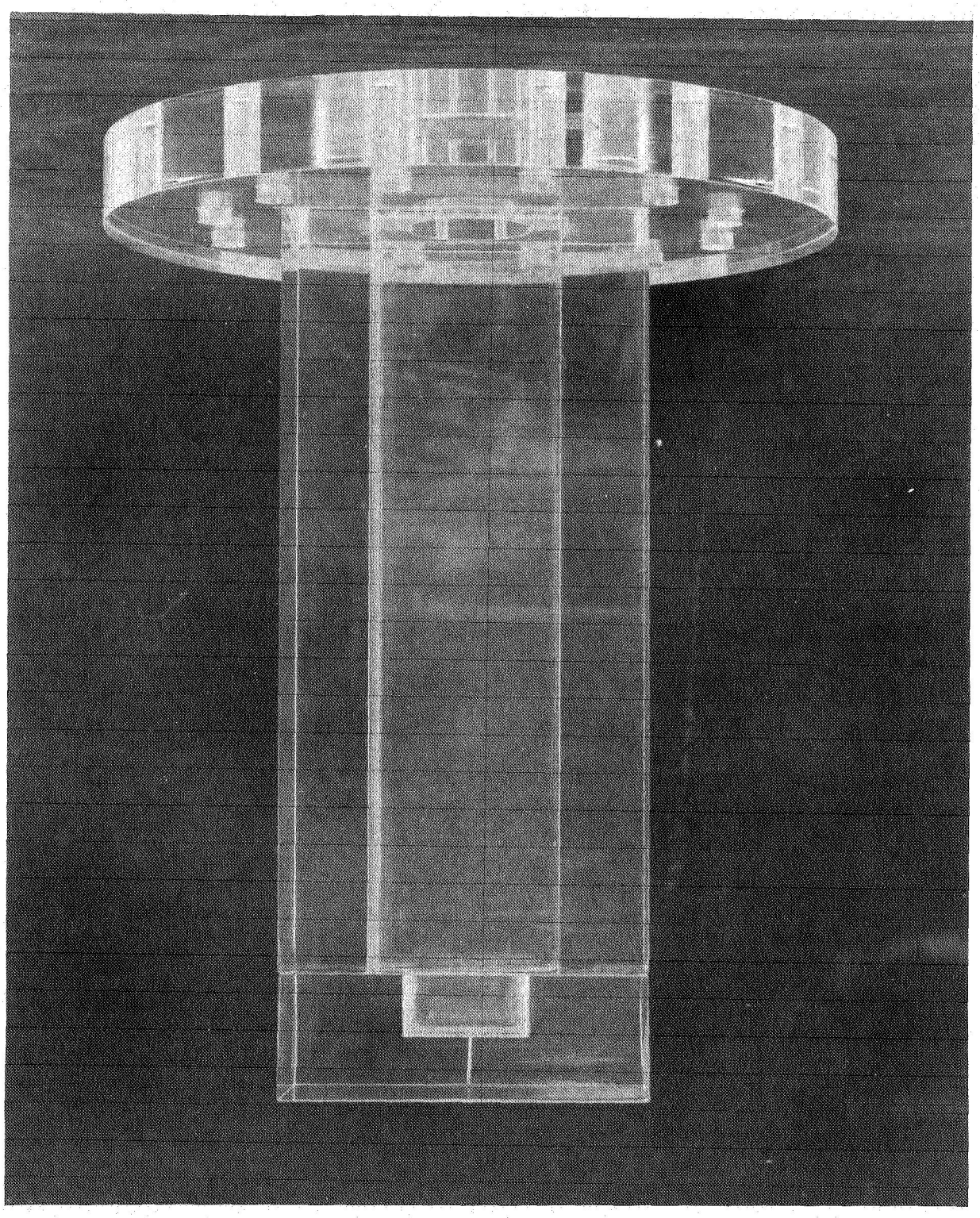

FIGURE 11(j)
Plexi-Glass Test Dewar (Specimen #7)

MICRO-METEORITE PUNCTURE LEAKAGE STUDY TEST RESULTS
Flow Discharge Coefficient Vs. Approximate Hole Diameter
(See Table I)
Sheet Thickness = 0.010"
This hole may have been
partially plugged by bits of
foreign material in the LH2,
since they observed in the dewar
at test completion.
1.0
0.9
0.8
0.7
0.6
0.5
0.4
0.3
0.2
0.1
0
.002
0.006
0.010
0.014
0.018
0.022
0.026
0.030
0.034
0.038
0.042
0.046
Upstream Approx. Hole Diameter (in)

FIGURE 12

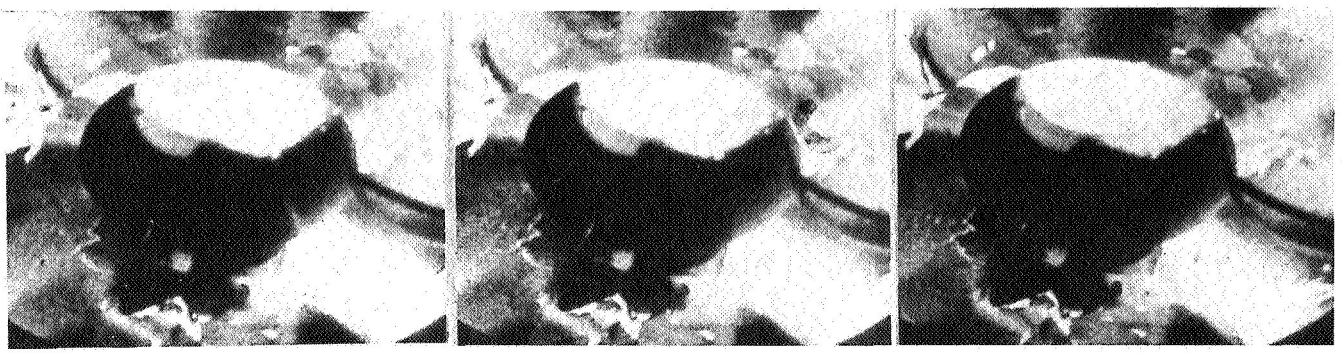

1 2 3

4 5 6

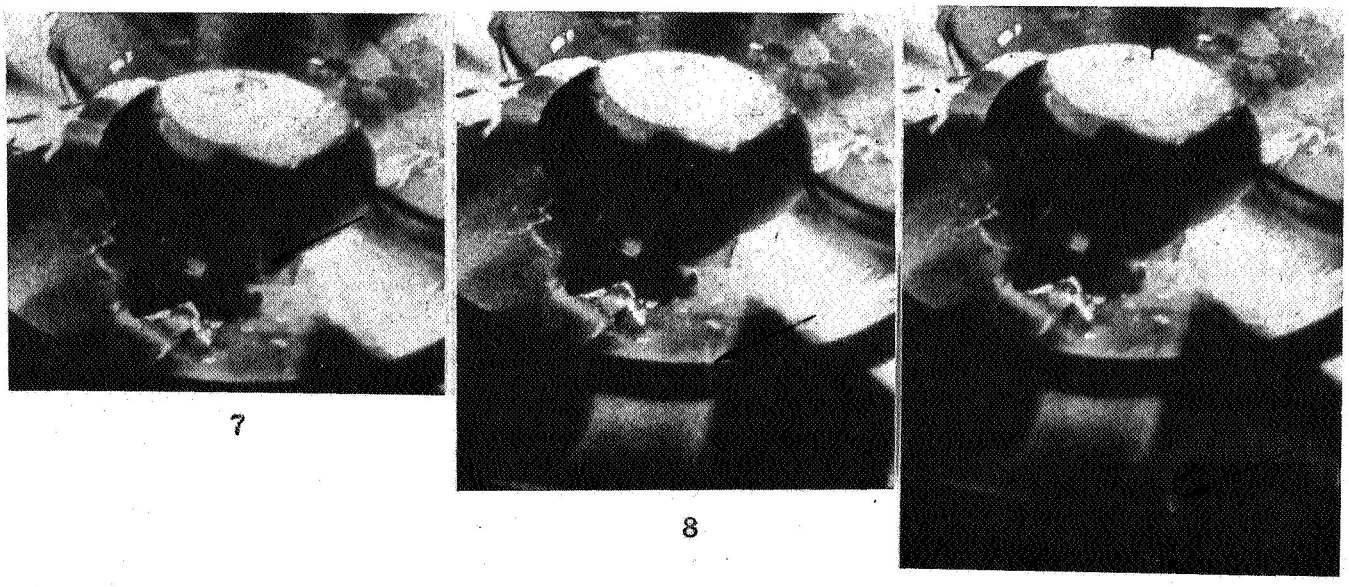

7 8 9

FIGURE 13
Specimen Puncture #5
(0.014 dia.)
Successive Frames at 128 fr/sec Showing Pellet Formation -
Arrow Shows Pellet Streak

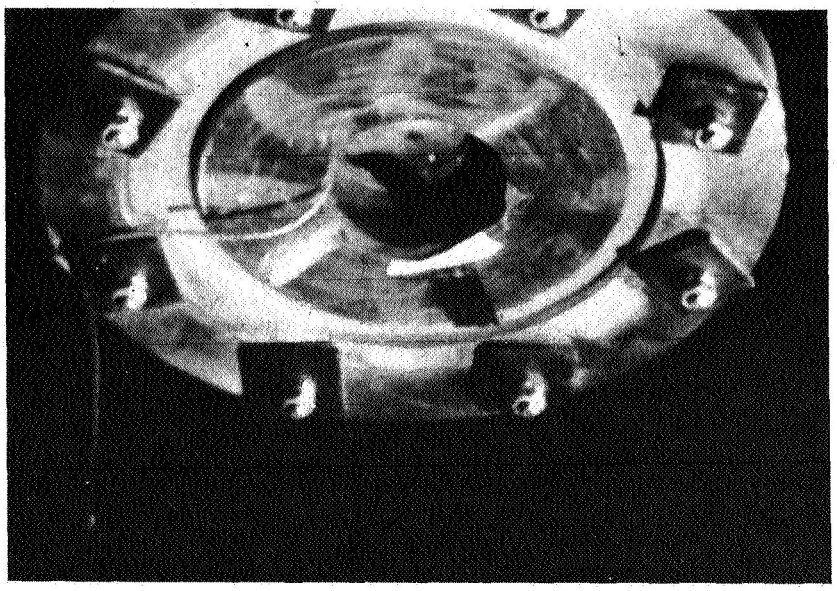

FIGURE 14
Pellet Formed From Specimen Puncture #5
(24 fr/sec)

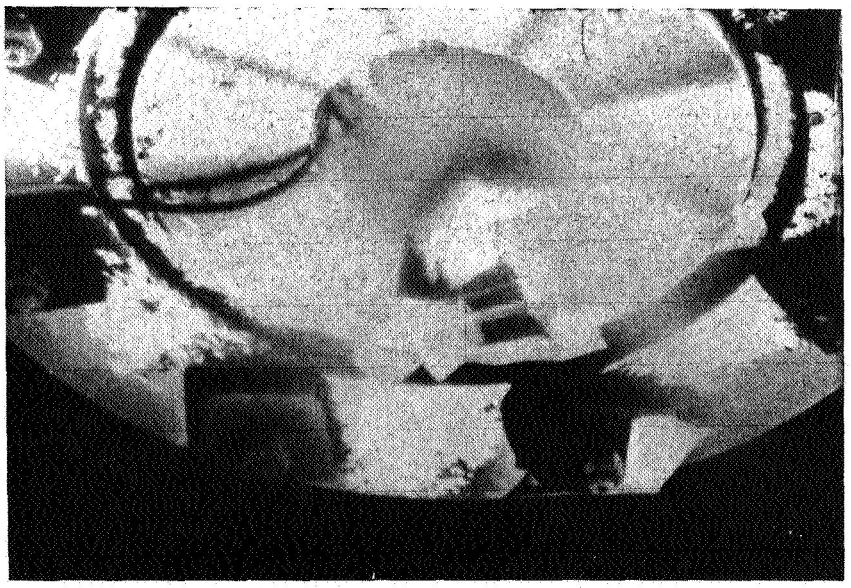

FIGURE 15
Spray From Specimen Puncture #6
Building Up Solid H_2 on Mylar Tape
(128 fr/sec)

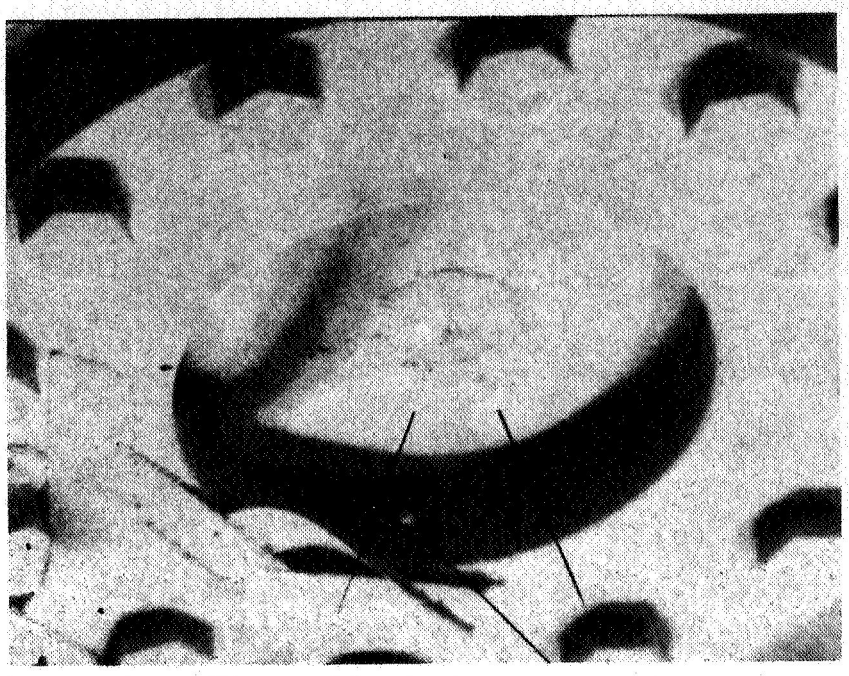

Figure 16
Pellet and Spray From Specimen Puncture #3 (0.020" dia)
Arrow Indicates Pellet, Lines Show Spray Cone (400 fr/sec)

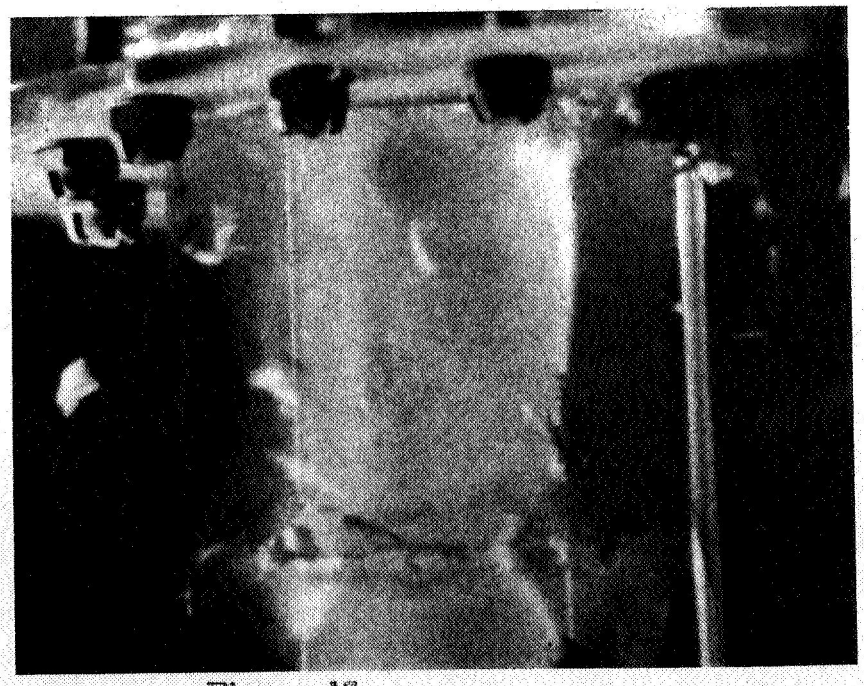

Figure 17
Solid N_2 Being Extruded From Cracks in a 3/4" Wall Plexiglass Dewar
(400 fr/sec)

IV. CONCLUSIONS AND RECOMMENDATIONS

The need for an understanding of the freezing phenomena associated with the free expansion of a cryogenic liquid or a cold gas to a state where the pressure is below its triple point pressure has occurred for specific configurations in the design of the Centaur vehicle and will continue to occur frequently in the design of vehicles which are designed to operate in the space environment. The areas of experimental investigation discussed in this report represent only a small sample of the situations where this freezing phenomena should be taken into consideration in the design. Perhaps many designers are not aware of the problems which could arise which will affect the operation of mechanisms under these conditions. For example, freezing in vehicle vent lines or the solid leakage past liquid propellant relief valves in space could cause propellant tank overpressurization or seriously affect the operation of sophisticated vent devices such as the "zero-g" liquid-gas separator for the Centaur fuel tank.

There is a great need for basic research to determine basic properties of the solids produced such as thermal conductivity, surface thermal resistance, heat capacity, etc. and many other properties or characteristics not normally determined such as what makes the solid stick to or unstick from a surface. These are needed in order to be able to analytically determine if problems

exist in any configuration where freezing might occur. For the many possible problem areas, an infinite amount of testing could be done attempting to simulate conditions and hardware. Much more could be gained if sufficient basic research was done by groups with the necessary facilities and understanding of the phenomena. An example of such a group is the National Bureau of Standards at Boulder, Colorado.

The author has postulated the following description of the process which produces at equilibrium the observed form of the solid in the expansion: As the liquid expands through a hole, it first breaks up into a myriad of tiny droplets. A fraction of the liquid on the droplet surface vaporizes, using the remaining liquid in the droplet as the source of the required heat of vaporization. The result is that most of the liquid in each droplet freezes. The size of the droplet is a function of the pressures which control the expansion. If the size of the hole is sufficiently small, the distance between the solid particles thus produced is small and they will collide with one another thereby producing larger sized particles which could accumulate in pockets and crevasses along the walls of the hole. In this manner the crystalline extrusions which were observed could be formed.

Because this is only conjecture, it is recommended that further basic experiments be performed to determine exactly what is taking place and to establish definitely the basic governing parameters.

From a quantitative point of view, the results of the thermodynamic analysis in the appendix appeared to agree very nearly with the observed phenomena. That is, under the test conditions it appeared that approximately 80% of the liquid escaping through the hole was frozen by the vaporization of the other 20%.

V. REFERENCES

1. Sheppard, J. J., "Investigation of Recovered Fragments from Atlas 109D Booster", GD/A Report AE62-0558, Unclassified, July 1962.

2. Jazwinski, A. H., "Fuel Losses on a Typical 6.2 Hour Centaur Mission Due to Meteoroid Puncture", GD/A Report AE61-1042, Unclassified, 28 August 1961.

3. Jazwinski, A. H., "Fuel Losses on a Typical 6.2 Hour Centaur Mission Due to Meteoroid Puncture, Addendum: Variable Flight Time", GD/A Report AE61-1042 Addendum, Unclassified 12 December 1961.

4. Jazwinski, A. H., "Meteoroid Puncture of Space Vehicles with Application to Fuel Losses on the Centaur", GD/A Report AE62-0453, Unclassified, 29 May 1962.

5. Rolsten, R. F., Hunt, H. H., and Welnitz, J. N., "Study of Principles of Meteoroid Protection", GD/A Report AE62-0413, Unclassified, April 1962.

6. Gallaher, W. H., "Investigation of Recovered Fragments from Atlas 109D Booster - Supplemental Information", GD/A Report AE62-0828, Unclassified, 14 September 1962.

7. Gallaher, W. H., and Sibulkin, M., "Investigation of Atlas Fragments Recovered in Brazil", GD/A Report AE62-0797, Unclassified, 20 August 1962.

VI. APPENDIX

A. Thermodynamic Analysis of Freezing Phenomena

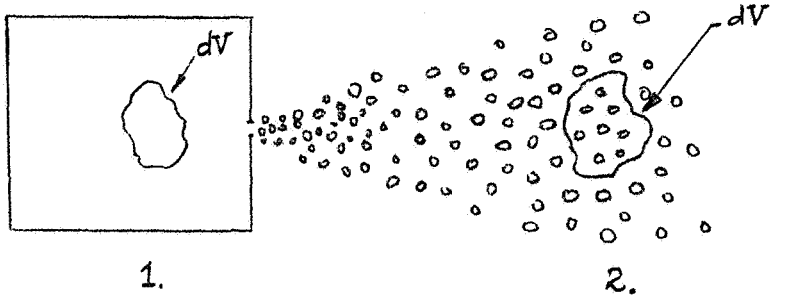

System: Elemental volume dV of constant mass;

A closed system in two states:

State 1) A liquid and/or a gas

State 2) A solid and/or a gas

Assumptions: (1) perfectly free expansion (to absolute zero pressure; P2 = 0)

(2) thermal equilibrium between the system and its surroundings

(3) velocity effects can be neglected

First Law of Thermodynamics for a closed System:

$$Q_{1-2} - Wu(1-2) = \Delta U_{1-2} \qquad (1)$$

but, $Q_{1-2} = 0$. This is after the walls are chilled to the liquid temperature. The expansion is so rapid that there is not time for significant heat transfer from the surroundings.

$W_{u(1-2)} = 0$ There is no work done on or by a free expansion.

Therefore $\Delta U_{1-2} = 0$ (2)

or $U_1 = U_2$ (total internal energy is unchanged)

but $U_1 = U_{g_1} + U_{l_1} = (Mu)_{g_1} + (Mu)_{l_1}$

and $U_2 = U_{s_2} + U_{g_2} = (Mu)_{s_2} + (Mu)_{g_2}$

or $(Mu)_{g_1} + (Mu)_{l_1} = (Mu)_{s_2} + (Mu)_{g_2}$ (3)

To put equation (3) in a more useable form, add and subtract

$M_{g_2} u_{s_2}$ and $M_{g_1} u_{l_1}$

$M_{g_1} u_{l_1} - M_{g_1} u_{l_1} + M_{g_1} u_{g_1} + M_{l_1} u_{l_1} = M_{s_2} u_{s_2} + M_{g_2} u_{g_2} + M_{g_2} u_{s_2} - M_{g_2} u_{s_2}$

or $M_{g_1} (u_{g_1} - u_{l_1}) + u_{l_1} (M_{l_1} + M_{g_1}) = M_{g_2} (u_{g_2} - u_{s_2}) + u_{s_2} (M_{s_2} + M_{g_2})$

but $M_T = M_{l_1} + M_{g_1} = M_{s_2} + M_{g_2}$

and $u_{g_1} - u_{l_1}$ = Internal energy heat of vaporization at state (1)

$= \Delta u_{v_1}$

$u_{g_2} - u_{s_2}$ = Internal energy heat of sublimation at state (2)

$= \Delta u_{s_2}$

$u_{l_1} - u_{s_2}$ = pseudo-internal energy heat of fusion

$= \Delta u_{f(1-2)}$

THEREFORE:

$$M_{g_1} (\Delta u_{v_1}) + M_T (\Delta u_{s(1-2)}) = M_{g_2} (\Delta u_{s_2}) \quad (4)$$

If it was all liquid at state 1, $M_{g_1} = 0$

then $$\frac{M_{g_2}}{M_T} = \frac{\Delta u_{f(1-2)}}{\Delta u_{s_2}} \quad (5)$$

since $u = h - \frac{pv}{J}$; $\Delta u = \Delta h - \frac{\Delta(pv)}{J}$

$$\frac{M_{g_2}}{M_T} = \frac{\Delta h_{f(1-2)} - \frac{\Delta(pv)_{f(1-2)}}{J}}{\Delta h_{s_2} - \frac{\Delta(pv)_{s_2}}{J}} \qquad \frac{\Delta h_{f(1-2)}}{\Delta h_{s_2}}$$

To solve for $\frac{M_{s_2}}{M_T}$, add and subtract $M_{s_2} u_{g_2}$ and $M_{g_1} u_{l_2}$

to equation (3)

then $u_{l_1} (M_{g_1} + M_{l_1}) + M_{g_1} (u_{g_1} - u_{l_1}) = M_{s_2} (u_{s_2} - u_{g_2}) +$

$u_{g_2} (M_{g_2} + M_{s_2})$

or $$M_{g_1} (\Delta u_{v_1}) + (M_T (\Delta u_{v(1-2)}) = M_{s_2} (\Delta u_{s_2}) \quad (6)$$

if $M_{g_1} = 0$,

$$\frac{M_{s_2}}{M_T} = \frac{\Delta u_{v(1-2)}}{\Delta u_{s_2}} \qquad \frac{\Delta h_{v(1-2)}}{\Delta h_{s_2}}$$

B. Micro-Meteorite Puncture Leakage Study Test Fixtures Development Problems

The pyrex glass and stainless steel dewar which serves as a reservoir and allows the liquid head above the hole specimens to be visually observed was the major item requiring special construction. The major parts are a 6" I. D. pyrex pipe approximately 2 ft. long sealed on the ends with 1" thick 321 stainless steel flanges. The necessity of being able to observe the liquid above the hole was shown in the general freezing phenomena tests. It was believed that gas pockets in the lines and not the freezing caused the flow fluctuation, but with an opaque apparatus, it could not be determined.

The major problem in construction of the dewar was to obtain a glass-to-metal seal which would have negligible leakage up to at least 100 psi $\triangle P$ across the seal and still be compatible with liquid hydrogen temperatures. This was obtained with highly finished contact surfaces and the use of thin (0.015" thick) teflon seals which were loaded in compression by approximately 4000 lbs. Because the pyrex glass will sustain very little shear load, a special loading mechanism was conceived and built which loaded the glass in almost pure compression. Allowances had to be made for the change

in dimensions and properties of the materials used at LH_2 temperatures.

The dewar was pressure tested with H_2O at atmospheric conditions and pressure tested by the liquid boil-off at LN_2 and LH_2 temperatures. The dewar was found to have negligible leakage under these conditions. Photographs taken during the development are shown in Figures 18 and 19.

The need for such a reservoir was expressed by others involved in experimental testing and should find use in subsequent tests.

Other problems which had to be overcome were (1) the "Bourdon tube effect" of the attached flex-hoses used for fill and vent lines. (The hoses tended to straighten out when pressurized. This was overcome by placing them opposite each other, thus causing them to cancel each other's effect.) (2) the variation in jet thrust with dewar internal pressure produced by the expanding liquid. This was effectively kept to a minimum by insulating the dewar from the heat source (the vacuum tank).

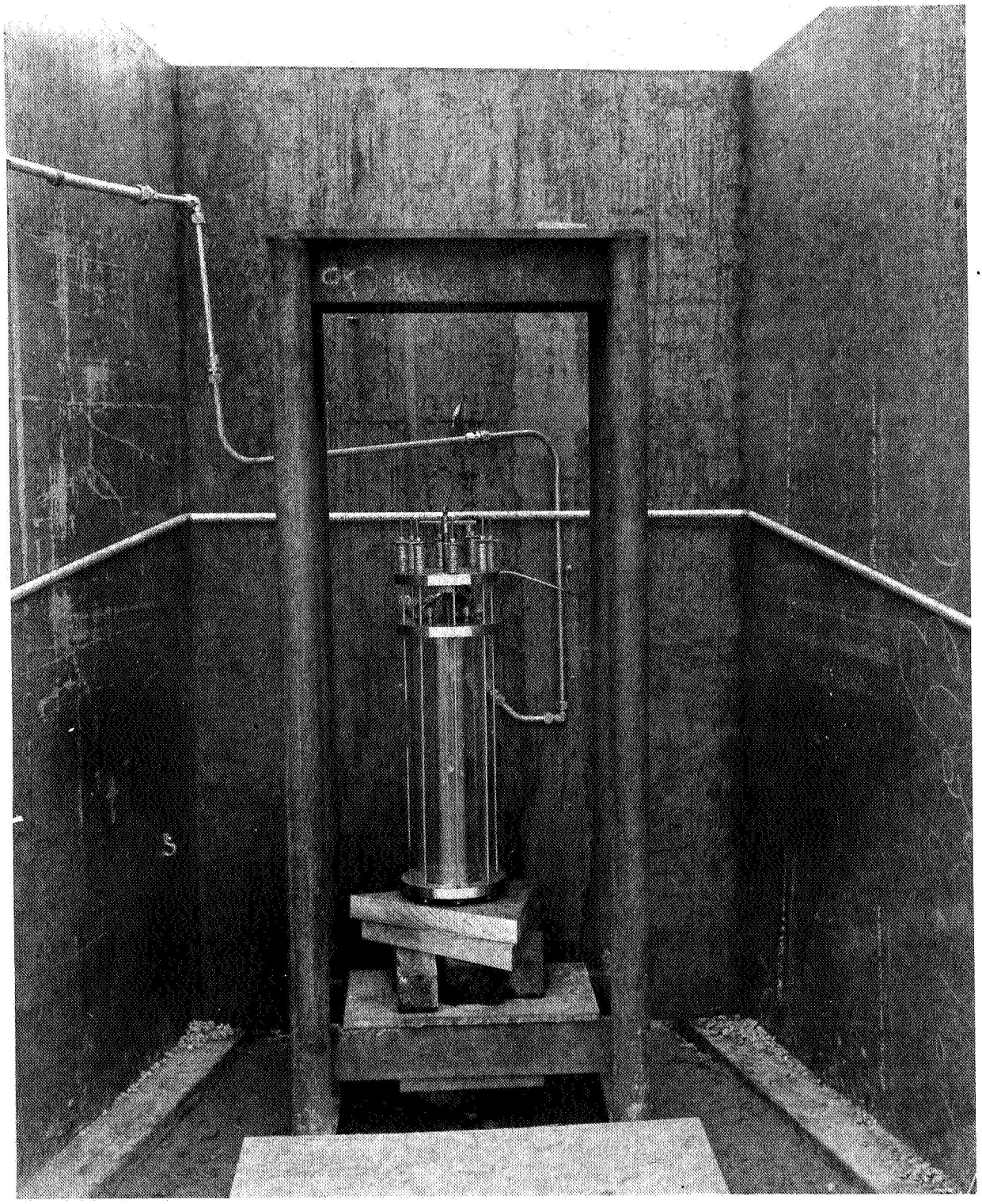

FIGURE 18
Pressure Proof Testing Set-Up With LH_2 & LN_2

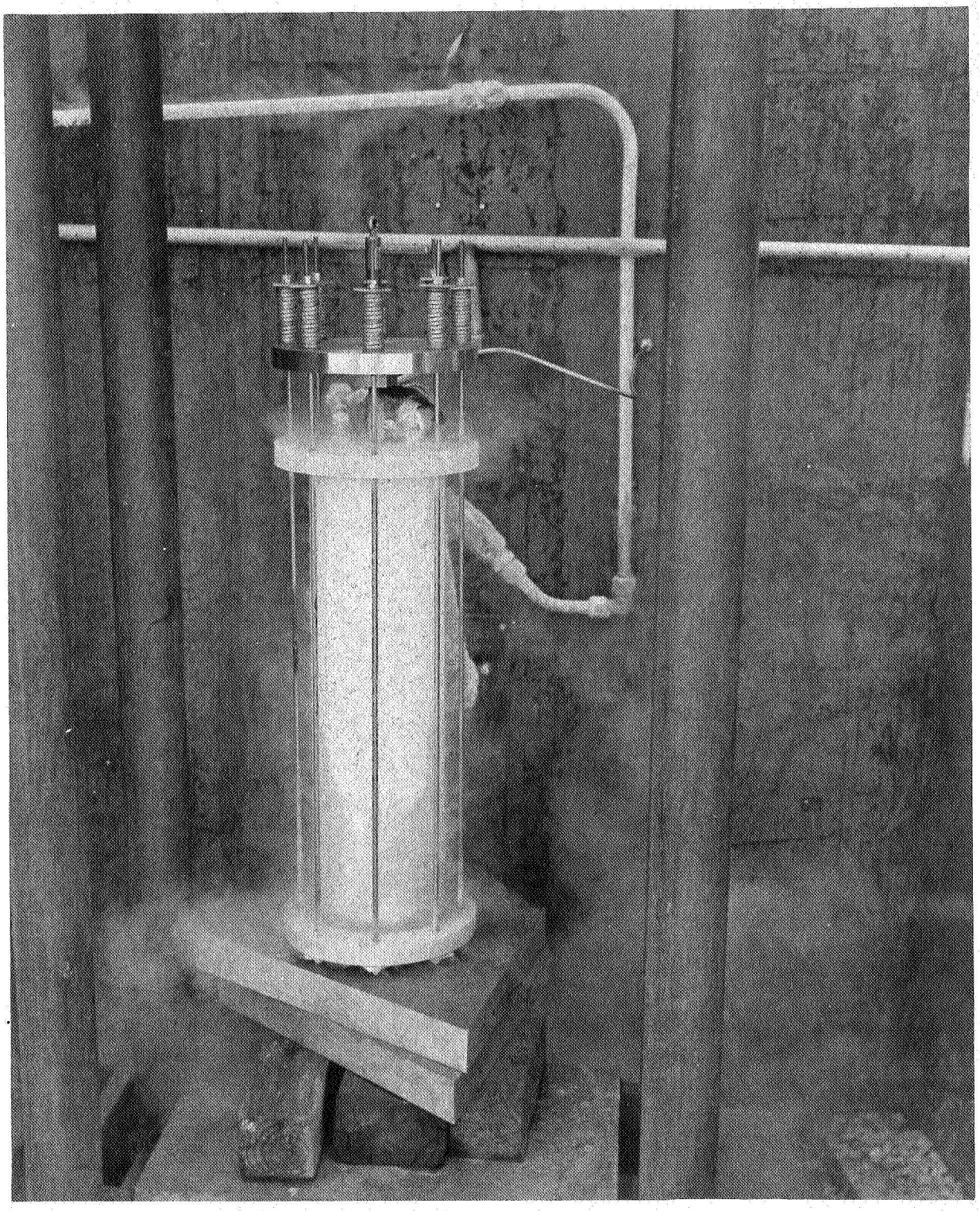

FIGURE 19
Pressure Testing With LH_2

GENERAL DYNAMICS

Convair Division